BIG – Branschsamverkan i grunden

Forskningsprogram för effektiv och säker grundläggning av vägar och järnvägar

Projekt A2017:10

Effects of climate change on slopes in sensitive clay

Final report for project

CHALMERS UNIVERSITY OF TECHNOLOGY

KTH

TRAFIKVERKET

STATENS GEOTEKNISKA INSTITUT

LULEÅ TEKNISKA UNIVERSITET

BIG – Branschsamverkan i grunden
Forskningsprogram för effektiv och säker grundläggning av vägar och järnvägar

Rapport BIG projekt A2017:10

Effects of climate change on slopes in sensitive clay

Final report for project

Carolina Sellin

CHALMERS

Framtagen inom ramen för BIG av Chalmers Tekniska Högskola

Stockholm 2021

Rapport publicerad av BIG, Branschsamverkan i grunden

Beställning Web: www.big-geo.se

ISBN 978-91-986926-2-4
Upplaga Digital

Framtagen av Chalmers Tekniska Högskola
Departement of Architecture & Cvili Engineering
Geology & Geotechnics
Författare Carolina Sellin

Foreword

This report summarizes the work that has been performed within the framework of BIG Project A2017-10 (TRV 2016/106280). That includes my initial doctoral studies as well as contributions from Minna Karstunen, Mats Karlsson, Jelke Dijkstra, Eleni Gerolymatou and Alexandros Petalas at Chalmers University of Technology. The work has also been performed in collaboration with Carina Hultén, representative from Trafikverket.

The project has been funded by Trafikverket (Swedish Transport Administration) through the research programme BIG, Branschsamverkan i Grunden. The work was also done as a part of the Digital Twin Cities Centre that is supported by Sweden's Innovation Agency VINNOVA.

Carolina Sellin
Göteborg, April 2021

Contents

Foreword **i**

1 Introduction **1**

2 Soil strength and soil models **2**
2.1 Swedish practice 2
2.2 Yielding of natural soils 3
2.3 Mobilisation of strength under triaxial loading 3

3 Methods for the evaluation of slope stability **5**
3.1 Limit Equilibrium Method 5
3.2 Discontinuity Layout Optimization 5
3.3 Finite Element Limit Analysis 6
3.4 Finite Element Analysis 6
3.5 Discussion and comments 6
3.6 Probabilistic approach 7

4 Test excavation in soft Champlain Sea clay **8**

5 Comparison of calculation methods **11**

6 Proposed method for stability evaluation **12**
6.1 Chosen soil model 12
6.2 Initiation of current stresses and geometry 12
6.3 Identification of failure mechanism and safety factor 13
6.4 Implementation on soft soil from Göta River valley 14
6.5 Numerical instabilities and convergence analysis 16

7 Effect of the climate on slope stability and soil strength **18**
7.1 Vegetation and evapo-transpiration 19
7.2 Desiccation cracks 20
7.3 Surface erosion 20
7.4 Artesian pore pressure 21
7.5 Microscale destructuration 21

8 Conclusions **22**

Acknowledgments **22**

References **23**

Appendix I:
Carolina Sellin (2019). "On evaluating slope stability in sensitive clay -a comparison of methods through a case study". *Proceedings of the 27th European Young Geotechnical Engineers Conference*. Ed. by Deniz Ülgen et al. Bodrum, Turkey: Turkish Society for ISSMGE, pp. 249–254

Appendix II: Summary of laboratory tests

Appendix III:
Alexandros L. Petalas et al. (2019). Modelling of undrained shearing of soft natural clays. *E3S Web of Conferences* **92**.15001, 1–5. ISSN: 22671242

Appendix IV:
Will be published separately during 2021.

Appendix V: Results from numerical simulations

1 Introduction

The stability of slopes is a well-known subject introduced for more than a century ago, with pioneering work by e.g. Petterson (1916) and Hultin (1916). This led to development of well established calculation methods and the current national guidelines, in which the effect of climate is most often included as a variation of the (ground) water level. However, climate research show that the Nordic countries will suffer from increased average temperature, more precipitation and higher likelihood of intense precipitation. As seen in Figure 1.1, the mean temperature in Sweden is expected to increase by 2 °C to 6 °C by year 2100, and the yearly amount of precipitation will increase by up to 20 %. The increase is expected to be larger in the Northern parts of the country, as well as larger on the West Coast than East Coast (Swedish Meteorological and Hydrological Institute, 2019). This is changing the environmental loads on slopes, in addition to secondary effects such as drought, fire and extreme cycles of drying-wetting and freeze-thaw. These new climate loads, combined with the uncertainties of both climate impact and soil properties, may lead to unnecessary, costly mitigation measures or undetected risks for infrastructure and constructions.

The report compares four available methods for stability analyses, and discusses a new methodology for evaluating the stability of slopes, as an initial step for evaluating the effect of different climate scenarios on slopes stability. The report also presents climate scenarios which are likely to occur in relation to Swedish slopes and summarises international research on how these climate scenarios could affect the stability or the strength of the soil in the slope.

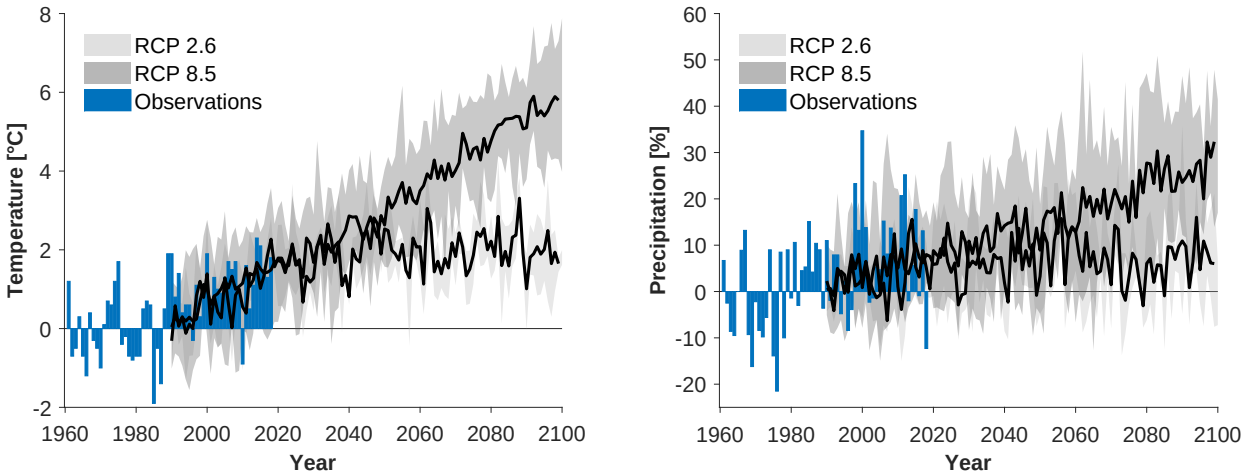


Figure 1.1: *Projected changes in annual mean temperature (left) and annual precipitation (right) in comparison to average value for the period 1961-1990. Black lines show the mean value from each emission scenario. Data collected from Swedish Meteorological and Hydrological Institute (2019).*

2 Soil strength and soil models

2.1 Swedish practice

The strength of a soil, in terms of slope stability, is by Swedish practice described with the *undrained* cohesion c_u, based on total stresses or *drained shear strength* expressed with effective stress parameters c' (the cohesion intercept) and φ' (the friction angle). The value of c_u is obtained from field or laboratory tests, such as vane tests, fall cone tests and CPTU. It is correlated to the depth or elevation where the field test is performed or where the soil sample is retrieved, corresponding to the *in situ* effective stress state. The value of c_u is by practice and recommendation corrected for the three test methods mentioned above with respect to the liquid limit, w_L, for the corresponding depth, see e.g. Larsson et al. (2007). The consistency of the soil, described with the liquid limit, is used to account for e.g. rate effects and anisotropy.

The mobilised shear strength is assumed to be a function of the depth or the elevation within a geological site, which imply that the soil strength is often treated as an one-dimensional concept dependent on (1) the experienced and current vertical effective stress and (2) the consistency of the soil, represented by the liquid limit. This approach is an adoption of the Mohr-Coulomb failure criterion (eq. 2.1), which assumes a perfectly-plastic behaviour of the soil:

$$\tau = c' + \sigma'_n \tan \varphi' \tag{2.1}$$

where τ is the mobilised shear strength and σ'_n is the normal effective stress at the plane of failure. By using Mohr-Coulomb failure criterion as a soil model, we assume that the shear strength parameters are constants and unaffected by any deformations and softening during extensive loading or failure. It is, therefore, impossible to do an estimation of strains or displacements in the soil before or after failure. The assumption of rigid-plastic behaviour until Mohr-Coulomb failure is used in Limit Equilibrium Method (LEM) for slope stability, which incorporates simplified static conditions along the failure surface, and is therefore unable to compute deformations in the soil.

Another simplification in using Mohr-Coulomb failure criterion as a soil model relates to its definition in three dimensions, with a hexagonal cone, where the intermediate stress is neglected, and thus does not influence the strength in the soil. This can be especially problematic simplification in complex slope geometries, where the stress state is truly three dimensional.

Moreover, when loaded soils may experience both (recoverable) elastic and (irrecoverable) plastic strains, depending on the whether the maximum previous stress is exceeded or not, as can be seen in an oedometer test. In terms of soil modelling, this is overcome by adding a 'cap', i.e. yield surface, to the failure criterion, and thereby distinguishing between small and large irrecoverable strains. An elastic-perfectly plastic model, such as Mohr-Coulomb, has a fixed yield surface, and does not predict the development of shear strength that can be noticed in e.g. direct simple shear test. As seen in Figure 2.1 and discussed by Muir Wood (1990), the soil underneath an external load experiences increasing deformations before it reaches failure, which means that the soil elements in (C) have reached beyond the measured peak strength (A) before failure. By assigning a constant value of the (peak) shear strength along a failure surface, the mobilised shear strength in point (B) and (C) will be overestimated, and any

influence of the inclination or direction of failure surface is ignored.

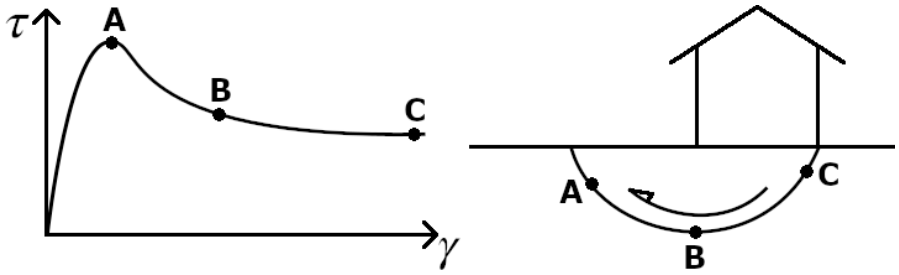


Figure 2.1: *Variation of mobilized shear strain along failure surface, where the shear strain, γ, is presented against the shear stress, τ. Adapted from Muir Wood (1990).*

2.2 Yielding of natural soils

A fixed yield surface or a failure criterion does not capture any evolution of the yield surface when the soil is subjected to varying loads. As can be seen from triaxial results in Figure 2.2, where each point represents the peak strength from a triaxial test, the dependence of yielding on effective stress level is noticeable. Therefore, a more comprehensive soil model should include expansion (hardening plasticity) and contraction (softening plasticity) of the yield surface when the soil is subjected to irrecoverable, plastic, strains. Hence, elasto-plastic models are constructed with four components; (1) an elastic law to describe the recoverable strains, (2) definition of yield criterion, to define a distinction between elastic and plastic strains, and implying the boundary between small and large strains, (3) a flow rule, to define the proportions of plastic strain increments, i.e. the ratio between the plastic volumetric and plastic shear strain increments, (4) a hardening rule, which defines the plastic strain increment.

An example of such a model is the Modified Cam Clay (MCC), introduced by Roscoe and Burland (1968). The formulation in MCC assumes an isotropic soil behaviour, which does not predict the anistropy seen in sensitive clay as a result of gravity, sedimentation, creep and/or previous loading history, apparent in Figure 2.2. It is also evident from experiments that the strength is affected by the stresses the soil is experiencing, the orientation of the stresses and the rate of which the stresses are applied. In addition, the apparent bonding between particles have proven to affect the strength. The constitutive model used in this project is the rate-dependent Creep-SCLAY1S model, which is hierarchically built from the MCC formulation, see e.g. Wheeler et al. (2003), Karstunen et al. (2005), Sivasithamparam et al. (2015), Gras et al. (2017) and Gras et al. (2018).

2.3 Mobilisation of strength under triaxial loading

An established method in Sweden for accounting the effect of anisotropy in Limit Equilibrium Method (LEM) is to divide the slip surface in three zones; "active" zone, direct shear zone and "passive" zone, referred to as ADP-zones, where each slice has one zone applied, based on the inclination of the base of the slice. The mobilized shear strength in the direct shear zone is thought to correspond to results from direct shear tests, and "active" and "passive" zone refers to peak strengths obtained from triaxial compression and extension test respectively. As

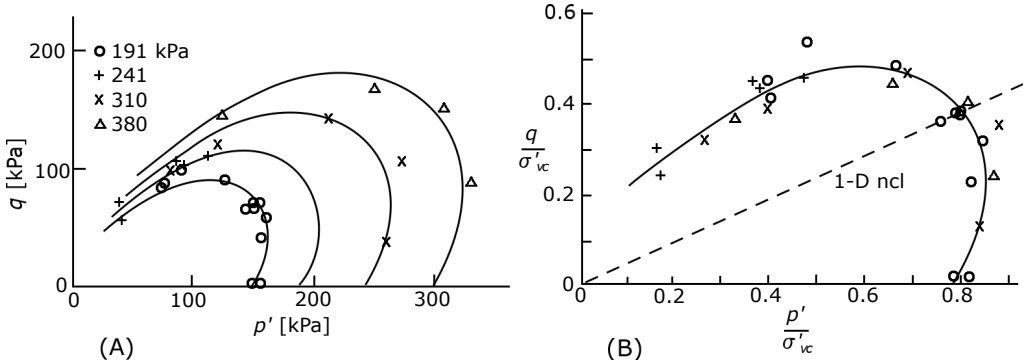


Figure 2.2: *Yield curves derived from triaxial tests performed on Winnipeg clay from four different depths. (A) Yield curves in mean effective stress-deviator stress ($p' - q$) space (B) yield curves normalised with preconsolidation pressure (σ'_{vc}). Adapted from Graham et al. (1983).*

discussed by Svahn (2015), however, the effect of applying ADP-zones gives varying results depending on the shape and location of the failure, as a steep slope with a steep failure mechanism will have a large number of slices acting in the "active" zone and few or none in the "passive" zone. On the contrary, a shallow slope will mainly include direct and "passive" zone along the slip surface. This kind of approach does not necessarily include the effect of horizontal effective stresses, and the rotation of the principal stresses on the mobilised shear strength, even if the inclination of the slice base is somewhat related to rotation of the principal stresses. Simulations of triaxial tests with varying OCR are shown in Figure 2.3, where an anisotropic model with stiffness degradation is used. As seen from the figure, the OCR and the respective K_0 affect not only the mobilised peak strength of the soil, but also the strain at the peak. The effective stress path is plotted in the mean effective stress-deviator stress ($p' - q$) space (left), axial strain ϵ_a vs deviator stress (middle) and ϵ_a vs the stress ratio q/p' (right). This highlights the importance of using a soil model that includes the effect of time and stress history, as well the effect of the direction of loading. The figure also shows the benefit of using a critical state model, where the ultimate strength, expressed as the critical stress ratio in compression M_c and in extension M_e, are independent of the chosen OCR and K_0.

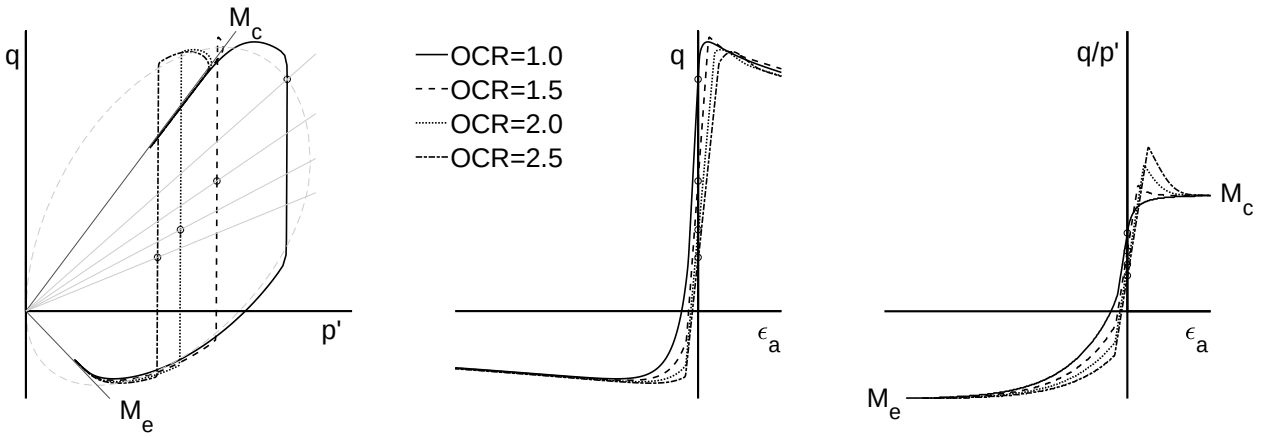


Figure 2.3: *Simulations of triaxial tests in compression and extension with different K_0-values, assuming the same horizontal effective stress. M_c refers to the slope of the critical state line in compression and M_e is the corresponding slope for extension.*

3 Methods for the evaluation of slope stability

New methods for calculation of slope stability have been developed during the recent years, as a result of research and increased computer capacity. Each method presented in the following has its advantages and disadvantages, even though one of the methods might be preferred as a result of tradition and simplicity, and the compliance with national guidelines and standards. An extensive guideline for slope stability calculations and the common mistakes in infrastructure project is presented by Finnish Transport Agency in the publication by Abed and Korkiala-Tanttu (2018). This chapter presents some methods for slope stability calculations that are available today.

3.1 Limit Equilibrium Method

The Limit Equilibrium Method (LEM) is the most commonly used method for slope stability, implemented in different forms over more than a century, by e.g. Hultin (1916), Bishop (1955) and Morgenstern and Price (1965). The method discretises an assumed sliding mass in to vertical slices for which force and/or moment equilibrium is calculated for each slice and the total mass. The value of the stability in LEM is then defined as the ratio of the shear strength along the slip surface over the shear stress for the same surface, called the Factor of Safety (FoS), as defined by Fellenius (1926). The benefit of the method is its simplicity, both computationally and logically. But the simplicity also result in some major drawbacks: (1) the shape and size of the failure surface is subjectively predefined by the user, (2) the mobilized shear strength for each slice is assumed to be constant (3) the method is mainly applicable for simple isotropic soil models, as it i not possible to account for changes in soil response (softening, hardening), even though possible add-ins for anisotropy are available. This could lead to an over- or underestimation of the stability, as well as the most critical slip surface may be overlooked.

3.2 Discontinuity Layout Optimization

Discontinuity Layout Optimization (DLO), similar to Finite Element Analyses (FEA), simulates the soil mass by discretizing it. In DLO this means representing the soil with a large number of sliding blocks. Similar to LEM, the equilibrium is dictated by the shearing between the blocks, but DLO is based on the upper bound theorem of plasticity (i.e. kinematics) rather than (stress) equilibrium. This means that the safety factor is described as the rate of work due to external loads over the simultaneous work done by internal stresses (Smith and Gilbert, 2007), similar to FEA. DLO is implemented in the software LimitState:GEO, where the safety factor can be obtained by either: (1) reducing the cohesion intercept, c', and the friction angle, φ' simultaneously, called *Adequacy on strength* or by (2) increasing the gravity in the model until failure, called *Adequacy on load*. The advantage of DLO compared to LEM is the independent search of the critical failure mode, both in terms of shape and location, where the number of sliding blocks is the main restriction. The disadvantage is that just like LEM, the mobilized shear strength is constant for each sliding block, and at the time of writing only static isotropic material models were available. As a conclusion, DLO is favourable over LEM for simplified slope stability calculations where non-circular failure modes are expected.

3.3 Finite Element Limit Analysis

Finite Element Limit Analysis (FELA) implements both the lower bound theorem (static equilibrium) and upper bound theorem (kinematic equilibrium) for a discretized soil mass, divided in to a mesh of finite elements (Sloan, 2013). By using finite elements, it is possible to account for a stress history in the soil mass. The (effective) stress state is used as input for the safety calculation, where an analysis is performed for each theorem, and the interval between them is narrowed down by increasing (automatically) the mesh density. The method is implemented in the software Optum G2/G3, where the safety factor is determined analogously to DLO, by either: (1) reduction of c' and φ', called *Strength Reduction* or (2) increase of gravity, called *Limit Analysis with gravity*. FELA is a simple but rigorous method for determining the critical failure mode, with the advantage of an independent search of the critical failure mode, similar to DLO. The drawback is the lack of possibility to include anisotropic or advanced soil models. The method, just like LEM, also offers some crude anisotropic formulations for total stress analyses.

3.4 Finite Element Analysis

Calculations of safety factor with Finite Element Analysis (FEA) are performed for a soil mass divided into a mesh of elements, where the response of each element is computed based on input data and the interaction with the surrounding elements. This is in contrast to DLO, where each block acts individually. In FEA, the failure mode is dictated by the material model and the (effective) stress state, resulting in a slip surface located where the mobilized shear strength is lower than the applied shear stress. This fulfils the both static and kinematic conditions simultaneously, in contrast to LEM, DLO and FELA. The safety factor is determined by either: (1) reducing c' and φ', available as a built in function in PLAXIS or (2) increasing the gravity, which is performed manually in PLAXIS. Note that c'-φ'-reduction requires a material model where these two parameters are defined, and is by definition not compatible with e.g. soil models sprung from Modified Cam Clay implemented as user-defined models. The advantage of FEA over FELA and the other methods previously mentioned is the ability to adopt advanced material models. Thus, the changes of effective stresses and the mobilized strength in the slope can be modelled as a function of time, or as a result of changing environmental conditions.

3.5 Discussion and comments

The safety factors dictated by the lower or upper bound theorems are clearly defined; the failure is obtained when no static or kinematic equilibrium can be achieved. This is similarly done in FEA, where the numerical procedure is performed until no equilibrium is achieved within certain number of iterations (Oberhollenzer et al., 2018). The safety factor is thereby very sensitive not only to the numbers of elements but also to the size of calculation increments, since this dictates when the stress path reaches the failure criterion. It is also worth noting that a gravity increase in FEA can possibly increase the strength of the material in effective stress analysis, potentially creating unrealistically high safety factors for shallow slopes when using Mohr-Coulomb model. This issue has been discussed by Swan and Seo (1999) and Hu et al. (2019).

As seen in the comparative study when using Mohr-Coulomb as failure criteria, presented in Appendix I, the failure mode and safety factor varies between the methods for small changes in the cohesion intercept c'. This implies uncertainties in the calculation methods, as well as emphasises the importance of choosing an appropriately justified value for c'. In addition, LEM and DLO gives the least conservative result for effective stress analyses, thus there is the need for considering other methods. The results also highlight the danger of implementing advanced climate-scenarios in calculation methods with built-in assumptions of failure mode, or indeed soil models without cap, as the safety factor varies substantially already without considering any climate scenarios.

3.6 Probabilistic approach

All geotechnical problems include parameters with different levels of uncertainties, e.g. external loads, surface geometry, ground water level, pore pressures, soil stratification, depth to bedrock, soil properties and model parameters. Each uncertainty is originating from one or both of the categories;

- Aleatory uncertainty: the natural variation of the soil.
- Epistemic uncertainty: the variation of human knowledge or practical handling of calculation tools, equipment and soil samples. This is something that can be reduced by education or research.

Determination of the strength of soil is a combination of both, as recognised by e.g. Wood (2016) and Christian et al. (1994). Thereby, the commonly used deterministic approach with a factor of safety only gives a partial representation of the actual safety margin (Lacasse, 2016). Both Eurocode with partial factors and Skredkommissionen (1995) include a safety margin and have varying target values of FoS depending on the consequence, where Skredkommissionen (1995) in addition favours the use of anisotropy and advanced laboratory tests. The partial factors of Eurocode, on the other hand, account for the natural variation of the soil parameter, the variety of test methods and sample distance, with a simplified probabilistic approach to include uncertainties in the soil parameters. Even so, neither of the methods assess the actual effect of soil variability on the factor of safety. Furthermore, with LEM we often assume a circular slip surface, which raises questions of both the reliability and the correctness of the failure mode. It is only by accounting for uncertainties in the soil that the risk level can be described (Lacasse, 2016).

An established method of dealing with uncertainties in slopes is by implementing the annual probability of failure, P_f, in comparison to the deterministic Factor of safety. The benefit of using P_f is that it can be combined with a consequence (e.g. monetary or life) to give a risk level, to be compared with a tolerable risk that society can live with. This has for instance been implemented in Australia, where Walker et al. (2007) suggest the annual tolerable risk for loss of life should be 10^{-4} for existing slopes standing minimum 10 years and 10^{-5} for new slopes, either man-made or modified. These threshold values should not be compared with the Swedish regulations based on FoS, since any relation between P_f and FoS from LEM is site-specific, as discussed by Lacasse (2018).

4 Test excavation in soft Champlain Sea clay

Even though failures of sensitive clays slopes and cuts made in sensitive clays are common, there are not many well-documented case studies. A test excavation was performed in August 1986 in soft clay, located approximately 40 km east of Montreal, Canada (Lafleur et al., 1988). The excavation measured 60 x 60 m on the surface and was 8 m deep, where each slope was respectively 18°, 27°, 34° and 45° to the horizontal. The purpose was to investigate the applicability of effective stress analyses to the design of cuts in sensitive clays.

The soil consisted of 0.6 m sand followed by a 1.8 m layer of fissured clay. A homogeneous clay layer extended to approximately 33 m depth resting on till. Sampling showed thin, discontinuous sand lenses, but results from piezometers showed no indication of a draining layer. The excavation was performed in two stages during one month; firstly down to 4 m depth, followed by a second excavation down to 8 m depth. The slopes were instrumented with, in total, 34 piezometers, located at several depths for each slope in the toe, the middle, the crest and 30 m from the crest. In addition, the two most shallow slopes (18° and 27°) had each 3 horizontal total pressure cells installed at 2 m depth.

Movements were recorded during the excavation in the 45° slope, and after excavation also in the 34° and 27° slope. The 18° slope remained intact during the test period of 1 year, as presented in Figure 4.1. The failure pattern was similar for each case; starting with visible cracks at the crest of the slope followed by a minor, shallow slip. A major failure followed a few days later, stretching to the toe of the slope, see Figure 4.1. The upper 2-3 m of the slip surface was vertical, corresponding to pre-existing tension cracks. Witnesses on the site describe that the slides occurred within seconds. The triggering was suspected to be related to the inclination of the slopes rather than climate conditions, since the first sign of failure in the three slopes was roughly inversely proportional to the inclination of the slope; the 45° slope started to fail day 0-2, the 34° on day 7 and the 27° slope on day 26.

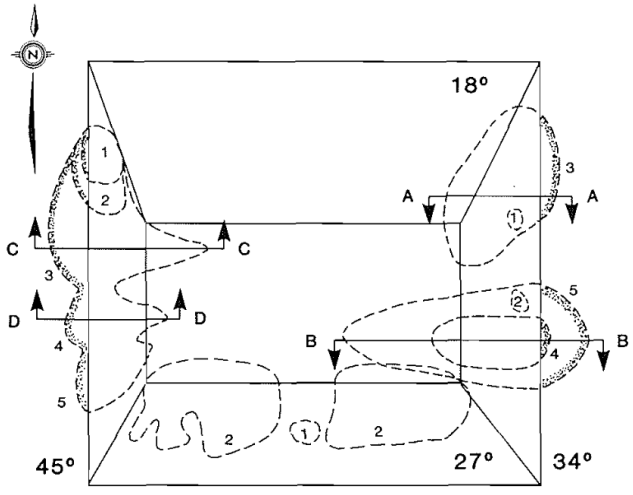


Figure 4.1: *Design of test site. Dashed lines with numbers indicate the areas of movement and their chronological order. From Lafleur et al. (1988).*

Back-calculations were performed for the 34° and 45° slopes with total and effective stress analyses with Bishops simplified method using LEM. The undrained strength parameters were taken as the minimum values from vane tests obtained before excavation and reduced by approximately 15%. The effective stress analyses were performed with c'=6 kPa and φ'=28°, as proposed as lower-bound values for Canadian marine clay in previous literature. The pore pressure distribution was based on the field measurements.

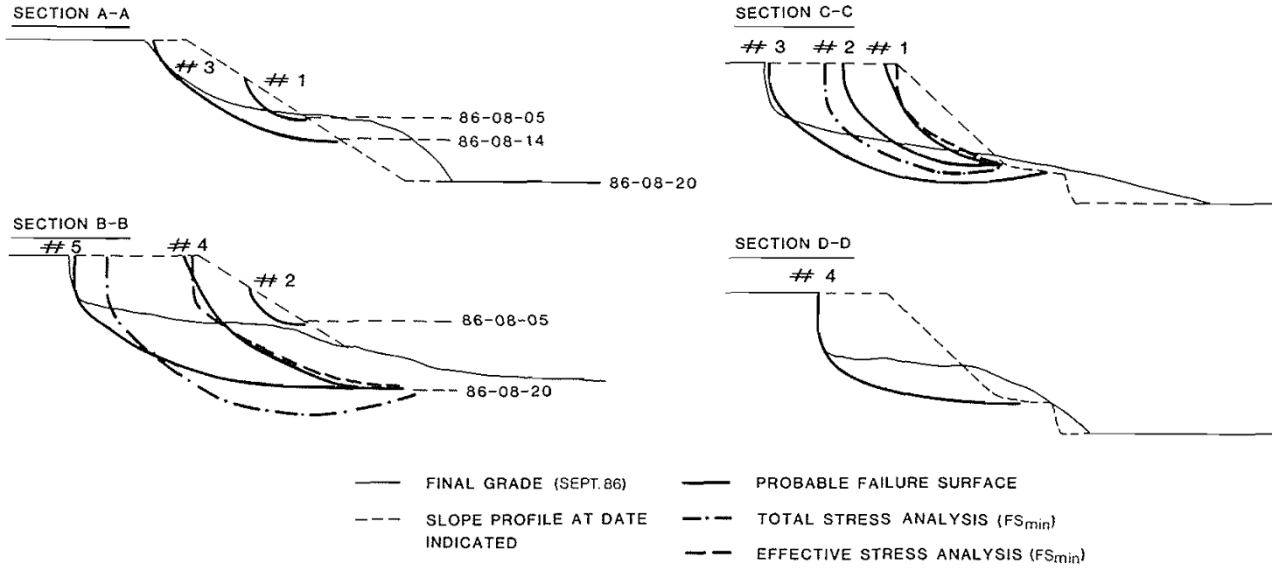


Figure 4.2: *Documented movements and corresponding back-calculations. From Lafleur et al. (1988).*

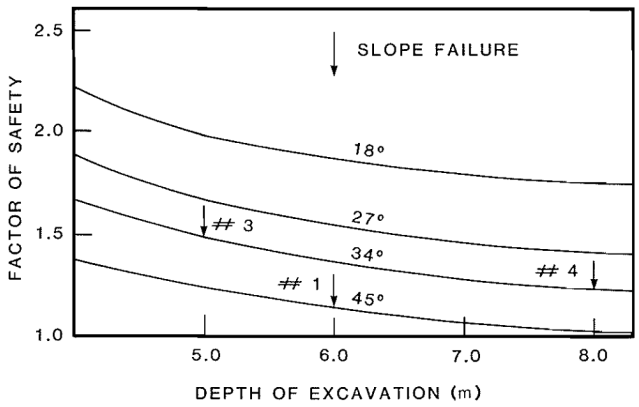


Figure 4.3: *Results from total stress analyses for varying depth and inclination of the slopes. Arrow indicate the registered slope failure in the test excavation. From Lafleur et al. (1988).*

The result presented in Figure 4.2 show that the calculated slip surfaces from the total stress analyses does not capture the initial, shallow failures, as well as the effective stress analyses. As the failures occurred within seconds, it might be tempting to adopt undrained, total stress analyses, but the calculations presented in Figure 4.3 show that results from total stress analyses overestimate the stability of the slopes that failed. Even though the failures were rapid, there were continuous changes in the pore-water pressures as a result of the excavation and the related deformations. It is evident that the total stress analyses, based on peak values

of undrained shear strength, do not reflect the actual soil behaviour. Instead, the effective stress based approach in combination with measured pore-water pressures at the moment of failure predicts the failure mechanism much better.

The conclusion of the paper is that even if failure occurred in just a matter of seconds (implying an "undrained" scenario), the failure is connected to the pore pressure changes occurring due to the excavation. Steady-state, or long-term conditions pore pressures occurred 5 months after the excavation of the cut, and all failures occurred before that. The main outcome of the experiments is the importance of accurate pore pressure assumptions, even for an apparent case of undrained stability.

5 Comparison of calculation methods

A geological site located approximately 12 km north of central Gothenburg was chosen to study different methods for slope stability analyses. The area is situated along Göta River and was thoroughly investigated during the planning and design process of the motorway E45 and the adjacent railway Vänerbanan. Figure 5.1 shows the chosen geometry, with hydrostatic pore pressure distribution and an assumption of no dry crust. The free water level was assumed to be at level -4, in order to create a critical slope scenario for the simulations. Further details on the geological conditions are found in Appendix I and II.

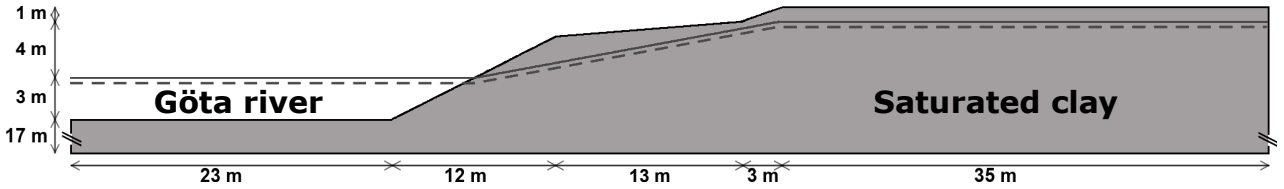


Figure 5.1: *Chosen geometry and ground water level of the cross section. Note: The model is horizontally cropped.*

The stability of the slope was investigated with four methods; LEM, DLO, FELA and FEA with Mohr-Coulomb failure criteria as soil model with both total- and effective stress based analyses. The critical failure mechanism in DLO, FELA and FEA was identified by using either reduction of the shear strength, c'-φ'-reduction, or by increasing the gravity in the model. Full results are presented in Appendix I.

The main outcome of the study was that all results from the total stress analyses showed similar failure mechanisms and safety factors. There was, however, a larger discrepancy between the results for effective stress analyses, where the non-FE-based methods, LEM and DLO, consistently showed the highest safety factors. This implies an inconsistency in the applications of the calculation methods. Sensitive clays are brittle materials that display strain-softening under undrained shear deformation, which may lead to the development of a progressive failure in the slope. Thus, we need to understand the effects of the soil stiffness, the rate of strain-softening and the residual resistance on the propagation of failure. In order to account for the complex stress history and state in a slope, an effective stress based method with representative constitutive model is needed, as deformations before the failure could affect the failure mechanism.

By using FE-based methods, the static and kinematic equilibrium are automatically fulfilled, and the failure mechanism can automatically develop in the weakest zone of the slope, regardless of the shape. In addition, by using increased gravity, the soil strength parameters are kept intact, and the failure mode is naturally triggered by the increase in soil weight and pore pressures. The c'-φ'-reduction, on the other hand, has the risk of affecting the failure mode when the strength parameters are reduced. It is therefore highly recommended to use increased gravity to simulate slope failure, even with a simple elasto-plastic soil model, such as Mohr-Coulomb.

6 Proposed method for stability evaluation

A new approach for slope stability evaluation is under development to overcome the shortcomings discussed in chapter 5. The proposed method is compatible with hydrological, hydrogeological and/or temperature simulations within fully coupled stability analyses. The analyses are done with PLAXIS 2D finite element code using the anisotropic rate-dependent soil model Creep-SCLAY1S.

6.1 Chosen soil model

Creep-SCLAY1S is an hierarchically formulated extension of the well-established elasto-plastic strain hardening model Modified Cam Clay (MCC) using critical state theory. The extension SCLAY1 accounts for both initial and evolving anisotropy, where the initial anisotropy includes both a rotation of the yield surface as well as allowing the yield surface to have a non-circular shape in the deviatoric plane. The evolving anisotropy on the other hand is represented by a strain-dependent reduction of the rotation through a separate rotational hardening law, in addition to the hardening law already formulated in MCC (Wheeler et al., 2003). The following SCLAY1S also includes bonding between particles in the soil and its destructuration during plastic strains, represented by a third hardening law (the destructuration law) with an initial bonding estimated from the sensitivity of the soil (Koskinen et al., 2002). Finally, Creep-SCLAY1S includes rate-dependency and adds a creep component to all strains during loading/unloading. As so, creep is included for both elastic and plastic strains, which is an acceptable simplification for normal consolidated or slightly overconsolidated soils. The creep component is dictated by a constant rate of a visco-plastic multiplier which is scaled by the rate of the relation between a current stress surface (CSS) and the corresponding stress surface for normal consolidated soil (NCS) (Sivasithamparam et al., 2015). It should be noted that the contribution of creep in the elastic range, when CSS is inside NCS, is very small.

Appendix III presents a comparison between the performance of MCC, SCLAY1S, with and without destructuration, and Creep-SCLAY1S for undrained triaxial tests on undisturbed samples taken in Gothenburg. As seen, the inclusion of anisotropy and destructuration in the simulation captures the recorded strain softening in the samples. A more thorough theoretical background to Creep-SCLAY1S is found in e.g. BIG Project A2015-06 with the report Amavasai and Karstunen (2017).

6.2 Initiation of current stresses and geometry

The rotation of principal stresses has substantial effect on the mobilised soil strength when using an effective stress based anisotropic rate-dependent soil model. It is therefore important to simulate the stress state correctly in a slope scenario, starting from the specific geological or man-made origin. This chapter focuses on a common scenario where a slope was created either slowly by natural erosion or fast by excavation.

The first step in any FE analyses of slope stability is the creation of the initial stress state. This can be done by so-called gravity loading, which results in a stress state that is in the equilibrium, but does not allow to account for the effects of overconsolidation in the starting value of K_0, the coefficient of earth pressure at rest. Thus, the resulting initial horizontal

stresses are erroneous. Alternatively, we can start with K_0 procedure, creating the in situ stresses with assuming appropriate K_0, assuming the soil layers to be horizontal. The current stress state in the slope is then created by a gradual unloading (erosion) with a simultaneous lowering of the water table, as seen in Figure 6.1. The initial calculation phase (phase 0) consist of a horizontal ground- and groundwater level. Both ground- and water level are then gradually lowered during calculation phase 1-5, and thereafter only the ground level is continuously lowered (calculation phase 6-8) until the final slope geometry is reached at phase 8. Details of the assigned hydraulic conditions are found in Appendix III.

As the static and kinematic equilibrium are fulfilled throughout the calculation phases, the principal stresses are gradually changing with the calculation phases, as does the K_0. In addition, since Creep-SCLAY1S is an anisotropic elasto-viscoplastic model with bonding and bond degradation, the changes in effective stresses affect the state of the soil: the preconsolidation, anisotropy and the amount of bonding.

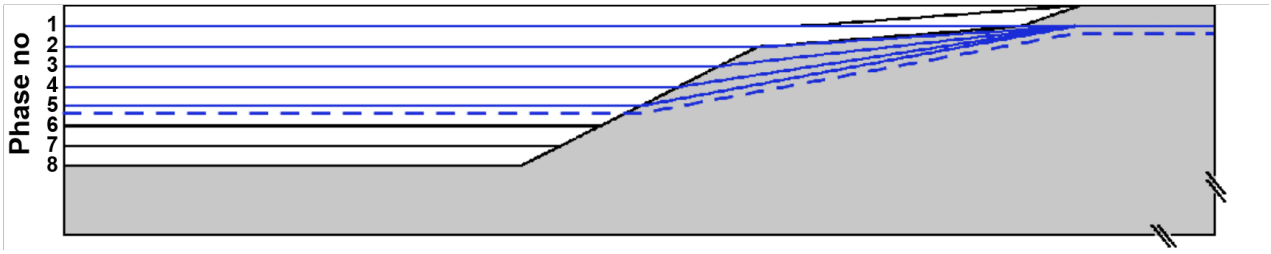


Figure 6.1: *Schematic view of coupled simulation of erosion process (black and blue lines) and ground water lowering (blue lines) that result in the final geometry.*

6.3 Identification of failure mechanism and safety factor

The failure mechanism using Creep-SCLAY1S in FEA is induced by a gradual increase of the gravity, regulated by the user who sets a target gravity that is larger than 1. It is recommended to perform a non-FE stability analysis before any advanced numerical simulations, as discussed by e.g. Abed and Korkiala-Tanttu (2018). The first target gravity can be selected as the Factor of Safety obtained from the non-FE analysis rounded up to next integer. The applied gravity in each calculation step is then dictated by (1) the target gravity, referred to as ΣM_{weight} in PLAXIS and (2) the calculation progress, ΣM_{stage}, with non-incremental steps from 0 to 1, where the number of steps is assigned by the user. The reached gravity and the equivalent Safety Factor, SF, is then calculated as:

$$SF = \Sigma M_{weight} \times \Sigma M_{stage} \tag{6.1}$$

The incremental increase of gravity is applied to the soil weight, and thereby gradually increases the excess pore pressure until the soil collapses and the slope reaches failure. ΣM_{stage} is thereafter constant in the remaining calculation steps due to the non-equilibrium situation in the model.

The value of SF should at this stage of method-development primarily be used as a tool for identifying failure mechanisms, investigating evolution of soil parameters over time in a slope

and comparing different scenarios in the same model. The method should not be used as a single tool for determining the safety factor of a slope, as discussed in the following.

6.4 Implementation on soft soil from Göta River valley

The same geological site as investigated in chapter 5 is revisited, with same (final) geometry. The slope is assumed to erode by 1m/10 years, as presented in Figure 6.1. Chosen soil parameters for Creep-SCLAY1S and their calibration against laboratory tests are found in Appendix III. Note that the soil parameters are assumed to be valid for a horizontal surface, as the soil samples were taken 15-30 m from the crest of existing slopes.

Figure 6.2 shows the result of the critical failure mechanism obtained by increasing the gravity in finite element analysis in combination with the soil model Creep-SCLAY1S. The target gravity was set to 2 with ΣM_{stage} set to 1000 steps, which resulted in a safety factor of 1.36. As seen in comparison with Figure 6.3, the failure mode align well between the total stress analyses with Mohr-Coulomb and the new method.However, the safety factors from the total stress analyses are 1.15 to 1.19 whereas the safety factor is significantly higher with FEA using Creep-SCLAY1S.

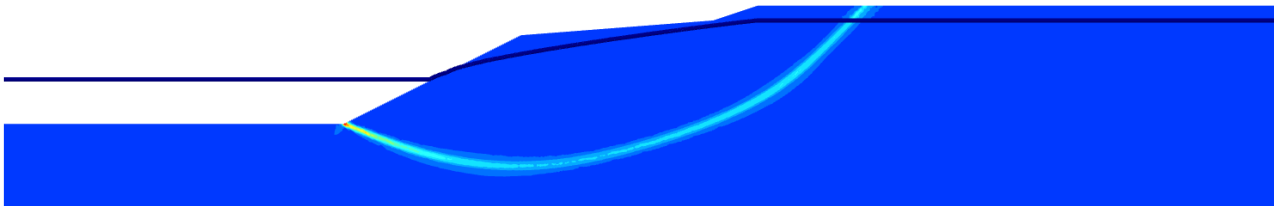


Figure 6.2: *Critical failure surface obtained by increasing the gravity, with a calculated safety factor of 1.36. The colour gradient represent the total shear strain, model horizontally cropped.*

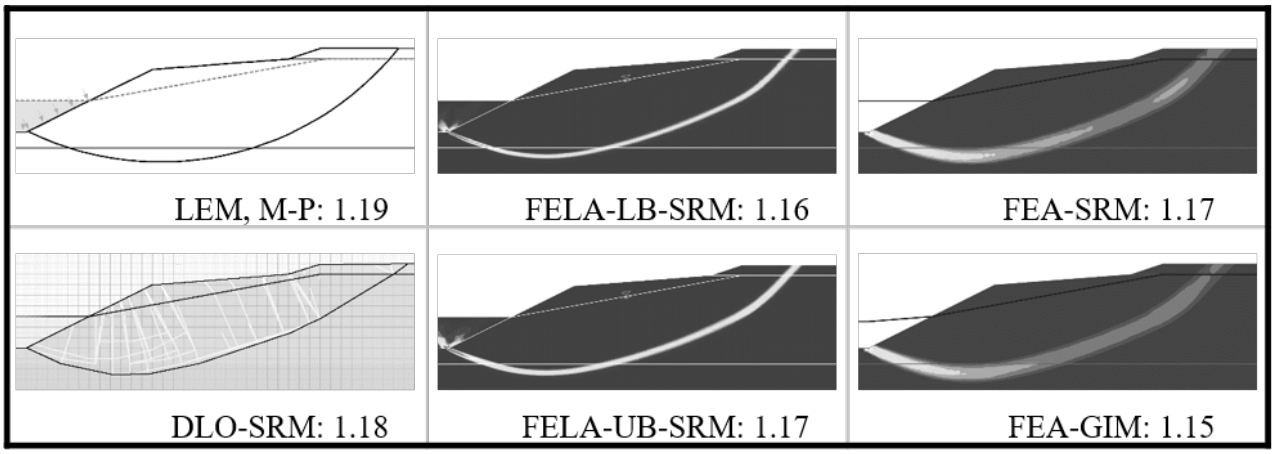


Figure 6.3: *Critical failure surfaces and safety factors from total stress analyses using Mohr-Coulomb, taken from Appendix I.*

The gradual erosion, before the safety calculation, give predictions of how the principal stresses rotate. For instance, in Figure 6.4, significant principal stress rotations are predicted below the unloaded (eroded) zone, as well as the corresponding K_0-values in Figure 6.5 have significantly increased. This affects the state of the soil, such as the size and the rotation of the Normal Compression Surface (NCS), leading to changes in the mobilised strength in these areas. As seen in Figure 6.6, a rotation of fabric in xy-direction, hence the rotation of NCS, is linked to the unloading and this is predicted to occur in the area where the failure is located. The effect of unloading to the other components of the fabric tensor (α_{xx}, α_{yy}, α_{zz}) can be found in Appendix IV.

The results highlight the importance of recreating the initial conditions of the slope before performing a safety analysis, as well as taking the site-specific stress situation into account when choosing a representative location for soil sampling.

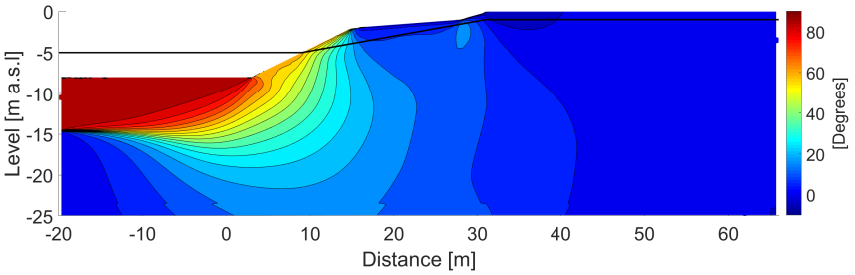


Figure 6.4: *Rotations of principal stresses.*

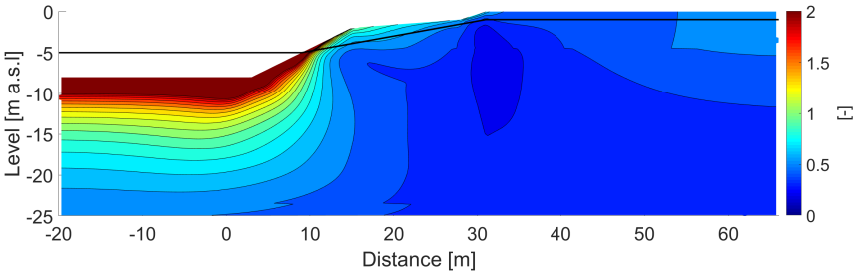


Figure 6.5: *K_0-values.*

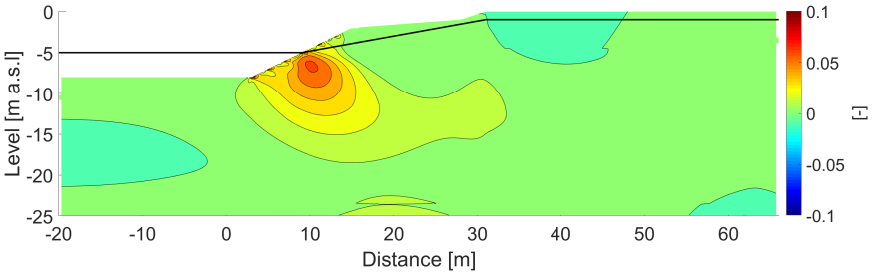


Figure 6.6: *Rotation of fabric tensor α_{xy}.*

6.5 Numerical instabilities and convergence analysis

Erosion process

The erosion process presented as essential for FE stability analyses of natural slopes with Creep-SCLAY1S includes assumptions of the rate of erosion, and how the slope geometry and water conditions evolved. The main disadvantage of this is the risk of generating unrealistic (negative) excess pore pressure during the erosion phases, which may affect the calculated stability. This is solved by adding a calculation phase after the last erosion step which reduces any excess pore pressure to maximum 1 kPa. The results from assuming 1 m erosion / 10 years, has also been compared with an identical model with 1 m erosion / 100 years, which gave very similar results in terms of both failure mechanism and safety factor. Thus, the rate of erosion does not seem to affect the stability.

Mesh density and computational time

The accuracy in a numerical model is dependent on the number and type of elements (degrees of freedom), and varies with the complexity of the geometry and the size of the model. In particular, the number of elements affect the width of the shear band (approx. 1 element wide), and consequently the obtained safety factor. The convergence analysis performed for the implemented slope, Figure 6.7, shows that the relation is non-linear. The author is therefore recommending a minimum of two mesh refinements to obtain a reliable result.Mesh sensitivity studies are most important when modelling problems involving failure.

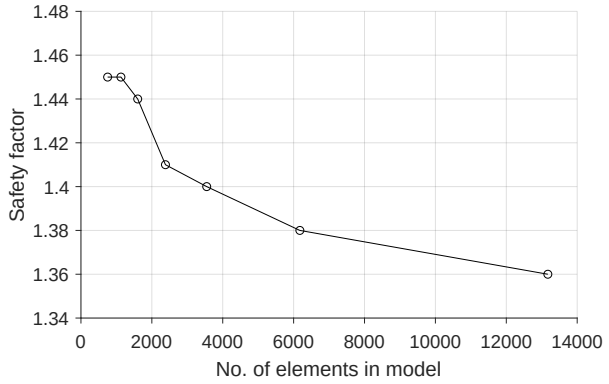


Figure 6.7: *Correlation between safety factor and mesh density for sample slope in Göta River valley.*

Number of nodes

The software used (i.e. PLAXIS) offers the option of performing calculations with 6 or 15 noded triangular elements. The choice affects the computational time, but may also affect the safety factor. A comparison for the slope used in this report was made with a coarse mesh with 6176 elements in the final geometry, using both 6 and 15 nodes. The computational time was reduced with 70% by reducing the number of nodes. In the latter case, however, no full shear band or failure mechanism was developed and the safety margin increased with more than 8%, which is an expected behaviour according to PLAXIS (2019b). Thus, not only the mesh density, but also the element type (and thus the number of degrees of freedom in numerical modelling the problem) is important.

Free-water and gravity

The increase of gravity in PLAXIS is applied differently on the steady-state pore water (long term) and the excess pore pressure (short term) (PLAXIS, 2019a). The steady-state pore water, such as hydrostatic pore pressure and free-water in rivers, is not increased incrementally with ΣM_{stage}, but instead reaches its final value in the first, initial calculation step. The excess pore pressure on the other hand, is dictated by the incremental increase of the soil weight, which is controlled by ΣM_{stage}. The effect of increasing the steady-state pore water all in on step is not fully investigated yet. A tempting explanation, however, is that the entire soil mass experience this drastic increase, therefore this does not result in any changes in the force equilibrium. On the other hand, the effect of a river as a resisting force might be overestimated with this method, as the final gravity, ΣM_{weight}, is not intended to be reached in the calculation.

7 Effect of the climate on slope stability and soil strength

The effects of the climate on the stability can be divided into direct and indirect effect on the stability. The clay affected will behave differently whether it is saturated or unsaturated. For instance, a direct effect of rainfall in the saturated zone results in an increase in pore pressure, whereas an indirect effect could be changes in the surface runoff followed by increased surface erosion. Likewise, a direct effect of increased temperature is loss of vegetation and an indirect effect is the loss of roots and their advantageous ductility and suction effects in the dry crust. As seen in Figure 7.1, the interaction between air, water and soil is essential to describe the effect of a changed climate. The scenarios presented in the figure are all based on marginally stable slopes of today, with large depths to bedrock and steep slope geometry.

The matrix presented in Figure 7.2 is an example of categorisation of cause and effect between isolated climate effects and their predicted impact on the stability of a slope. The row for *Geology and topography* refers to shallow slopes or slopes with shallow bedrock, further discussed in separate sub-chapter. The last row, *Vegetation*, is highly dependent on local conditions and even the local microclimate.

Internal erosion occurs primarily in situations with high water levels and extreme water flow within the slope. This is a rare phenomenon in sensitive clay in Sweden and will not be investigated further in this report. However, Tang et al. (2018) discuss the possibility to reduce the internal erosion by customizing the adjacent vegetation.

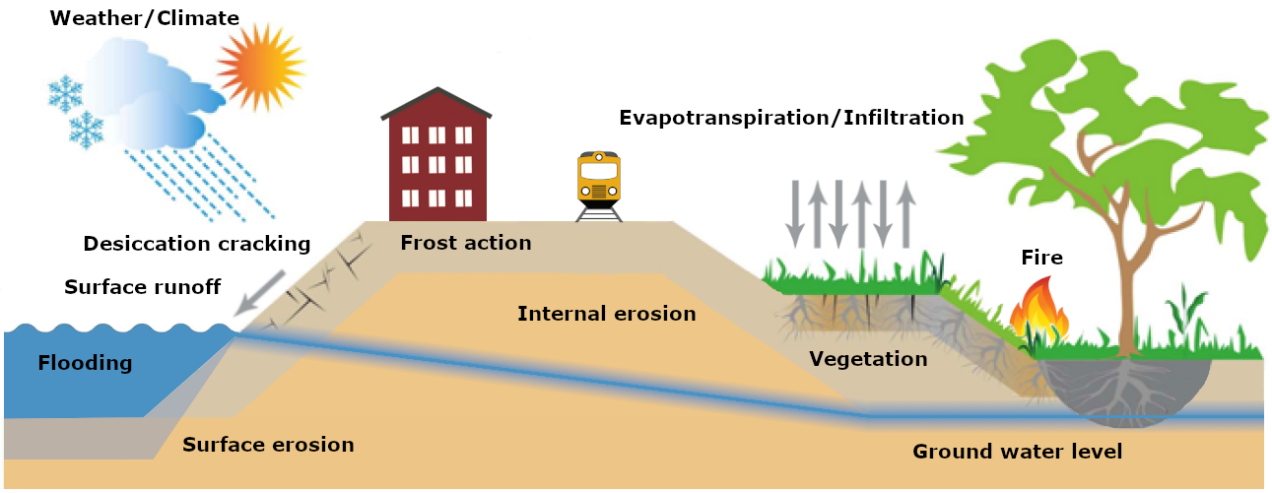


Figure 7.1: *Soil-climate-vegetation interaction posing hazards in slope stability, figure based on Tang et al. (2018).*

			Unsaturated zone / Dry crust			Saturated zone		
			Changed evotranspiration	Desiccation cracks	Surface erosion	Ground water level	Artesian pore pressure	Microscale destructuration
Environmental load	Precipitation	Flooding and increased river flow	(x)		x			
		Pore pressure changes	(x)	x		x	x	(x)
	Temperature	Surface runoff	(x)		x			
		Drought	x	x		x	x	x
	Cyclic changes	Drying - Wetting	x	x	o			x
		Freezing - Thawing		x	o			x
Local conditions	Geology and topography				x	x	x	x
	Vegetation		x	o	x	o		

Figure 7.2: *Correlation between environmental loads and their effects on slope stability parameters, divided into direct, X, and indirect, O, effects.*

7.1 Vegetation and evapo-transpiration

Evapo-transpiration is defined as the process of water brought to a vapour state either from a wet surface (evaporation) or from plants leaves (transpiration). The rate of the process is affected by e.g. temperature, wind and solar radiation, and the evapo-transpiration is expected to strongly increase in Northern Europe as a result of climate change (Tang et al., 2018).

The occurrence of vegetation (roots) in slopes contribute to both tensile strength and reduction of pore pressure via suction. The vegetation above the ground surface, however, also adds weight to the slope, including the risk of overturning trees, and during dry periods vegetation can both deepen and extend the desiccation cracks (Tang et al., 2018). The measurable effect varies with the plant species, the spatial orientation of the slope and the seasonal climate.

For instance, previous studies have shown that the tensile strength in roots from Scots pines varies with the season, in addition to the naturally grown Scots pines generating stronger roots than the planted pines (Genet et al., 2005). The seasonal change of the tensile strength is a likely a result of the water content in the roots, as the strength usually decrease with increasing diameter of the roots. In addition, as seen in the full-scale experiment performed by Glendinning et al. (2014), the spatial variation of the slope direction affects the evapo-transpiration and thereby the type of vegetation growth and its expanse. In the experiment, the southern slope experienced more sunlight and was more exposed to wind, resulting in a greater evapo-transpiration and thereby a greater drying, leading to a higher soil suction than the northern slope. These tendencies could increase with more extreme weather in the future, potentially leading to more extreme microclimates. The numerical study performed by Tsiampousi et al. (2017) suggest that the seasonal fluctuations of precipitation and potential

evapo-transpiration may reach deeper than the maximum root depth in the slopes of a road cut. The study also simulated low and high water demand vegetation in the slope, where a low water demand vegetation resulted in a reduction of the safety factor over time. Simulations of a high water demand vegetation instead, increased not only the safety factor, but also the vertical displacements.

7.2 Desiccation cracks

An effect of desiccation cracking is the risk of shallow, passive failures. This occurs after a dry season, when the cracks are filled with water, creating an increased horizontal stress. Previous experiments, such as Ng et al. (2003), show that the horizontal stress can become more than three times higher than the vertical total stress.

Increased rainfall is mainly affecting the dry crust and shallow part of the slope, and is especially a subject worthy for consideration for steep slopes. Several studies, such as e.g. Glendinning et al. (2014), notice that increased rainfall is affecting the pore pressure down to 1.5 - 2.0 m depth, corresponding to the depth of cracks and fissures. The full scale rainfall experiments performed by Ng et al. (2003) showed that the response in pore pressure, water content and horizontal stresses occurred with 1-2 days delay after initiation of an artificial rainfall. A majority of the effects occurred during the first 3 days, even though the slope was exposed for artificial rainfall during 7 days.

7.3 Surface erosion

The common effect of surface erosion on slope stability along rivers and shorelines is the gradual increase of slope gradient, as the slope is undercut by water flow and some of the weight at the toe is removed. In addition, periods of drought lead to temporary reduction in water infiltration, and thereby increasing the surface run off (Tang et al., 2018). As the drought also leads to deepening of desiccation cracks, the surface erosion is likely to increase. Studies also show that wildfires affect not only the vegetation and its canopy, but the additional top layer of ash and the intense drying of the soil itself also lead to a temporary increase in water repellency and thereby accelerating the surface erosion as well (Kinner and Moody (2008) and Cannon et al. (2010)).

7.4 Artesian pore pressure

An arising problem with increased precipitation could be the generation of artesian pore pressure in gentle slopes with small depths to bedrock. The increase of precipitation will lead to higher inflow to the bottom moraine, creating an increased pore pressure starting from the bottom of the clay layer. This increase of pore pressure close to the bottom moraine has been documented in Gothenburg, though unpublished, where the fluctuation in pore pressure is suspected to be related to local precipitation. A major problem with these slopes is the risk of them being overseen in conventional stability assessment, since they do not require a steep inclination. The proximity to bedrock could even be classified as a positive feature for the stability. Since this scenario is highly dependent on the local geology, a pragmatic approach is to identify these slopes by GIS-analysis with depth to bedrock, in combination with occurrence of clay and visible bedrock.

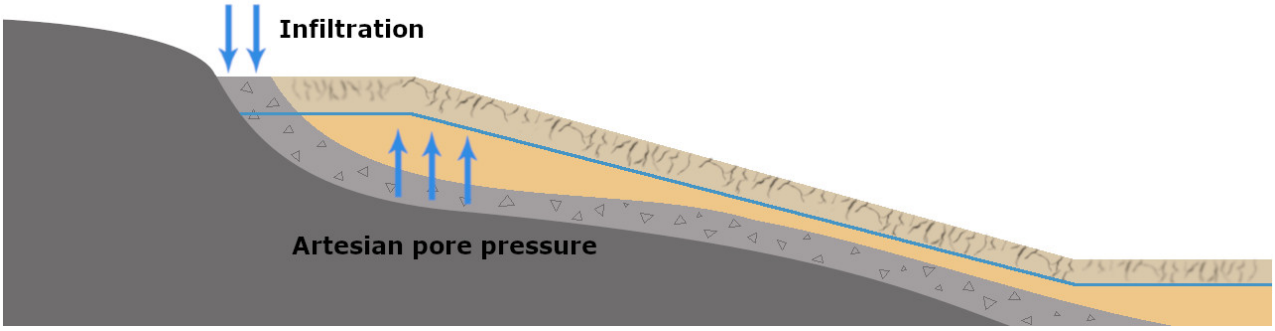


Figure 7.3: *Infiltration in bottom moraine leading to artesian pore pressure.*

7.5 Microscale destructuration

The soil response is dictated by many factors, such as loading history, water content and salinity, but it also fluctuates with temperature. As shown by Li et al. (2018), the effect of temperature changes in oedometer tests is related to the apparent bonding of the clay. This could have a long-term effect on soil strength, as well as the continuous cycles of drying-wetting and freezing-thawing of the soil. The depth of which the air temperature is affecting the soil varies with the thermal properties of the soil, and an increase of the annual air temperature is likely to increase the temperature through out the soil depth. The amplitude and frequency of the cyclic drying-wetting and freezing-thawing will also affect the soil. For instance, the study by Li (2019) shows that cyclic temperature changes are accelerating creep in sensitive clays, in addition to the acceleration of creep due to static increase of soil temperature. Some projections of freeze-thaw cycles for the Nordic countries show an increase of cycles in the Northern parts and a decrease in the South, although the transition between them is yet uncertain. Thus the changes in the amount of drying-wetting and freezing-thawing cycles may lead to yet unexpected soil response.

8 Conclusions

It is fundamental to use an effective stress based model in order to simulate and predict the effect of various climate scenarios on the stability of slopes, as the pore pressure is an essential parameter for determining the slope stability. This has been highlighted in e.g. the full scale experiment on Champlain Sea clay. The new method proposed in this report show the advantages of using effective stress FE analyses with an advanced soil model, where not only the failure mechanism is identified, but also the evolution of stresses and the corresponding soil response (e.g. anisotropy and destructuration). The results show that simulations of the stress history to reach the current stress state in a slope is just as important as the choice of safety analysis method. Likewise, visualizations of the current stress state show that undisturbed soil sampling should be performed at a notable distance from the slope crest, in order to avoid stress rotations in the sample and to be able to fully replicate the in-situ stresses in the laboratory. The method proposed also has the possibility to be further expanded to include effects from the climate, such as temperature, and the specific response in the unsaturated zone. Overall, the assumed initial conditions, with complex stress orientation and anisotropy, are essential for advanced slope modelling and for predicting slope stability for existing slopes and their evolution in a future climate.

Acknowledgments

The financial support from Trafikverket in the framework of BIG (Branchsamverkan i Grund) and is greatly acknowledged.The work is done as part of Digital Twin Cities Centre that is supported by Sweden's Innovation Agency VINNOVA.

References

Abed, Ayman and Leena Korkiala-Tanttu (2018). *Stability analysis for road-cutting Review, recommendations and examples*. DOI: 10.13140/RG.2.2.10562.02244 (cit. on pp. 5, 13).

Amavasai, Amardeep and Minna Karstunen (2017). *BEST SOIL: Soft soil modelling and parameter determination*. November. Gothenburg. ISBN: 9789198430103 (cit. on p. 12).

Bishop, Alan W (1955). The use of the Slip Circle in the Stability Analysis of Slopes. *Géotechnique* **5**.1, 7–17. ISSN: 0016-8505. DOI: 10.1680/geot.1955.5.1.7 (cit. on p. 5).

Cannon, Susan H., Joseph E. Gartner, Michael G. Rupert, John A. Michael, Alan H. Rea, and Charles Parrett (2010). Predicting the probability and volume of postwildfire debris flows in the intermountain western United States. *GSA Bulletin* **122**.1-2, 127–144. ISSN: 00167606. DOI: 10.1130/B26459.1 (cit. on p. 20).

Christian, John T, Charles C Ladd, and Gregory B Baecher (1994). Reliability Applied to Slope Stability Analysis. *Journal of Geotechnical Engineering* **120**.12, 2180–2207. DOI: 10.1061/(ASCE)0733-9410(1994)120:12(2180) (cit. on p. 7).

Fellenius, Wolmar (1926). Jordstatiska beräkningar med friktion och kohesion (adhesion) och under antagande av cirkulärcylindriska glidytor. *Kungl. Väg- och Vattenbyggarkåren 1851-1926, festskrift, Stockholm* 22/12, 79–127 (cit. on p. 5).

Genet, Marie, Alexia Stokes, Franck Salin, Slobodan B Mickovski, Thierry Fourcaud, Jean-François Dumail, and Rens Van Beek (2005). The Influence of Cellulose Content on Tensile Strength in Tree Roots. *Plant and soil* **278**.1, 1–9. DOI: 10.1007/s11104-005-8768-6 (cit. on p. 19).

Glendinning, Stephanie, Paul Hughes, Peter Helm, Jonathan Chambers, Joao Mendes, David Gunn, Paul Wilkinson, and Sebastien Uhlemann (2014). Construction, management and maintenance of embankments used for road and rail infrastructure: implications of weather induced pore water pressures. *Acta Geotechnica* **9**.5, 799–816. DOI: 10.1007/s11440-014-0324-1 (cit. on pp. 19, 20).

Graham, J., M. L. Noonan, and K. V. Lew (1983). Yield states and stress-strain relationships in a natural plastic clay. *Canadian Geotechnical Journal* **20**.3, 502–516. ISSN: 00083674. DOI: 10.1139/t83-058 (cit. on p. 4).

Gras, J-P, N Sivasithamparam, M Karstunen, and J Dijkstra (2017). Strategy for consistent model parameter calibration for soft soils using multi-objective optimisation. *Computers and Geotechnics* **90**, 164–175 (cit. on p. 3).

Gras, J-P, Nallathamby Sivasithamparam, Minna Karstunen, and Jelke Dijkstra (2018). Permissible range of model parameters for natural fine-grained materials. *Acta Geotechnica* **13**.2, 387–398 (cit. on p. 3).

Hu, Chang-ming, Yi-li Yuan, Yuan Mei, Xue-yan Wang, and Zheng Liu (2019). Modification of the gravity increase method in slope stability analysis. *Bulletin of Engineering Geology and the Environment* **78**.6, 4241–4252. ISSN: 1435-9537. DOI: 10.1007/s10064-018-1395-2 (cit. on p. 6).

Hultin, Sven (1916). Grusfyllningar för kajbyggnader. *Teknisk Tidskrift* **V.U.h**.31, 292–294 (cit. on pp. 1, 5).

Karstunen, Minna, Harald Krenn, Simon J Wheeler, Mirva Koskinen, and Rachid Zentar (2005). Effect of anisotropy and destructuration on the behavior of Murro test embankment. *International Journal of Geomechanics* **5**.2, 87–97 (cit. on p. 3).

Kinner, David A and John A Moody (2008). *Infiltration and runoff measurements on steep burned hillslopes using a rainfall simulator with variable rain intensities*. Tech. rep. U.S. Geological Survey Scientific Investigations Report 2007–5211, p. 64. DOI: 10.3133/sir20075211 (cit. on p. 20).

Koskinen, M, M Karstunen, and Simon J Wheeler (2002). "Modelling destructuration and anisotropy of a natural soft clay". *Proceedings of the 5th European Conference on Numerical Methods in Geotechnical Engineering*. Ed. by P Mestat. International Society of Soil Mechanics and Geotechnical Engineering. Paris: Presses de l'ENPC, Paris, pp. 11–20. URL: https://www.tib.eu/de/suchen/id/BLCP%7B%5C%%7D3ACN070381368 (cit. on p. 12).

Lacasse, Suzanne (2016). "Hazard, Reliability and Risk Assessment - Research and Practice for Increased Safety". *Proceedings of the 17th Nordic Geotechnical Meeting*. Reykjavik, pp. 17–42 (cit. on p. 7).

Lacasse, Suzanne (2018). *Reliability-based Design for Robust Geotechnical Practice. Stanley D. Wilson Memorial Lecture* (cit. on p. 7).

Lafleur, Jean, Vincent Silvestri, R Asselin, and M Soulié (1988). Behaviour of a test excavation in soft Champlain Sea clay. *Canadian Geotechnical Journal* **25**.4, 705–715. DOI: 10.1139/t88-081 (cit. on pp. 8, 9).

Larsson, Rolf, Göran Sällfors, Per-Evert Bengtsson, Claes Alén, Ulf Bergdahl, and Leif Eriksson (2007). *Skjuvhållfasthet - utvärdering i kohesionsjord*. 2nd. Linköping: Information 3. Swedish Geotehcnical Institute (SGI), p. 64 (cit. on p. 2).

Li, Yanling (2019). "On the impact of temperature perturbations on the creep of sensitive clay". Doctoral thesis. Chalmers University of Technology, p. 138. ISBN: 9789179051013 (cit. on p. 21).

Li, Yanling, Jelke Dijkstra, and Minna Karstunen (2018). Thermomechanical creep in sensitive clays. *Journal of Geotechnical and Geoenvironmental Engineering* **144**.11, 1–11. ISSN: 10900241. DOI: 10.1061/(ASCE)GT.1943-5606.0001965 (cit. on p. 21).

Morgenstern, N R and V Eo Price (1965). The Analysis of the Stability of General Slip Surfaces. *Géotechnique* **15**.1, 79–93. ISSN: 0016-8505. DOI: 10.1680/geot.1965.15.1.79 (cit. on p. 5).

Muir Wood, David (1990). *Soil behaviour and critical state soil mechanics*. Cambridge: Cambridge university press, p. 486. ISBN: 0521332494 (cit. on pp. 2, 3).

Ng, C W W, L T Zhan, C G Bao, D G Fredlund, and B W Gong (2003). Performance of an unsaturated expansive soil slope subjected to artificial rainfall infiltration. *Géotechnique* **53**.2, 143–157. DOI: 10.1680/geot.53.2.143.37272 (cit. on p. 20).

Oberhollenzer, Simon, Franz Tschuchnigg, and Helmut F Schweiger (2018). Finite element analyses of slope stability problems using non-associated plasticity. *Journal of Rock Mechanics and Geotechnical Engineering* **10**.6, 1091–1101. DOI: 10.1016/j.jrmge.2018.09.002. URL: http://www.sciencedirect.com/science/article/pii/S1674775518302129 (cit. on p. 6).

Petalas, Alexandros L., Mats Karlsson, and Minna Karstunen (2019). Modelling of undrained shearing of soft natural clays. *E3S Web of Conferences* **92**.15001, 1–5. ISSN: 22671242 (cit. on p. 35).

Petterson, Knut E (1916). Kajraset i Göteborg den 5:te mars 1916. *Teknisk Tidskrift* **V.U.h**.30 and 31, 281–287, 289–291 (cit. on p. 1).

PLAXIS (2019a). *Personal communication, 2019-11-15.* (Cit. on p. 17).

PLAXIS (2019b). *PLAXIS 2D Reference Manual CONNECT Edition V20* (cit. on p. 16).

Roscoe, K. H. and John Boscawen Burland (1968). "On the generalized stress-strain behavior of "wet" clay". *Engineering plasticity*. Ed. by J. Heyman and F. A. Leckie. Cambridge: Cambridge university press, pp. 535–609 (cit. on p. 3).

Sellin, Carolina (2019). "On evaluating slope stability in sensitive clay -a comparison of methods through a case study". *Proceedings of the 27th European Young Geotechnical Engineers Conference*. Ed. by Deniz Ülgen, Altuğ Saygili, Mehmet Rifat Kahyaoğlu, Selda Durmaz, Onur Toygar, and Aysu Göçügenci. Bodrum, Turkey: Turkish Society for ISSMGE, pp. 249–254 (cit. on p. 26).

Sivasithamparam, Nallathamby, Minna Karstunen, and Paul Bonnier (2015). Modelling creep behaviour of anisotropic soft soils. *Computers and Geotechnics* **69**, 46–57 (cit. on pp. 3, 12).

Skredkommissionen (1995). *Anvisningar för släntstabilitetsutredningar Rapport 3:95*. Linköping, p. 196 (cit. on p. 7).

Sloan, S W (2013). Geotechnical stability analysis. *Géotechnique* **63**.7, 531–572. DOI: 10.1680/geot.12.RL.001 (cit. on p. 6).

Smith, Colin and Matthew Gilbert (2007). "Application of discontinuity layout optimization to plane plasticity problems". *Proceedings of the Royal Society A: Mathematical, Physical and Engineering Sciences*. Vol. 463. 2086. The Royal Society. Royal Society, pp. 2461–2484. DOI: doi.org/10.1098/rspa.2006.1788 (cit. on p. 5).

Svahn, Victoria (2015). *Slopes in soft clay : management of strength mobilisation*. Göteborg: Chalmers University of Technology. ISBN: 9789175971988 (cit. on p. 4).

Swan, Colby C and Young-Kyo Seo (1999). Limit state analysis of earthen slopes using dual continuum/FEM approaches. *International Journal for Numerical and Analytical Methods in Geomechanics* **23**.12, 1359–1371. DOI: doi.org/10.1002/(SICI)1096-9853(199910)23:12<1359::AID-NAG39>3.0.CO;2-Y. (cit. on p. 6).

Swedish Meteorological and Hydrological Institute (2019). *Climate scenarios*. URL: https://www.smhi.se/en/climate/climate-scenarios/ (visited on 08/15/2019) (cit. on p. 1).

Tang, A. M. et al. (2018). Atmosphere-vegetation-soil interactions in a climate change context; impact of changing conditions on engineered transport infrastructure slopes in Europe. *Quarterly Journal of Engineering Geology and Hydrogeology* **51**.2, 156–168. DOI: 10.1144/qjegh2017-103 (cit. on pp. 18–20).

Tsiampousi, Aikaterini, L. Zdravkovic, and D. M. Potts (2017). Numerical study of the effect of soil–atmosphere interaction on the stability and serviceability of cut slopes in London clay. *Canadian Geotechnical Journal* **54**.3, 405–418. ISSN: 12086010. DOI: 10.1139/cgj-2016-0319 (cit. on p. 19).

Walker, Bruce, Warwick Davies, and Grahame Wilson (2007). Practice note guidelines for landslide risk management. *Australian Geomechanics Journal* **42**.1, 64–109 (cit. on p. 7).

Wheeler, Simon J, Anu Näätänen, Minna Karstunen, and Matti Lojander (2003). An anisotropic elastoplastic model for soft clays. *Canadian Geotechnical Journal* **40**.2, 403–418 (cit. on pp. 3, 12).

Wood, Tara (2016). "On the Small Strain Stiffness of Some Scandinavian Soft Clays and Impact on Deep Excavations". Thesis for the degree of Doctor of Philosophy. Chalmers University of Technology, p. 225 (cit. on p. 7).

Appendix I: On evaluating slope stability in sensitive clay -a comparison of methods through a case study

ON EVALUATING SLOPE STABILITY IN SENSITIVE CLAY -A COMPARISON OF METHODS THROUGH A CASE STUDY

Carolina Sellin, *Chalmers University of Technology, Architecture and Civil Engineering, carolina.sellin@chalmers.se*

ABSTRACT

This paper presents a comparison of four methods of analyses for slope stability for drained and undrained conditions with Mohr-Coulomb failure criteria, applied on a simplified slope along Göta River, Sweden. In addition to Limit Equilibrium Method (LEM), the methods include Discontinuity Layout Optimization (DLO), Finite Element Limit Analysis (FELA) and Finite Element Analysis (FEA), using both Strength Reduction Method (SRM) and Gravity Increase Method (GIM). The results showed very good correlation between all methods for undrained analyses, whereas the drained analyses showed a noticeable discrepancy in both the safety factor and the failure mode for small cohesion intercept between SRM and LEM. Results from the drained analyses performed with GIM were >100% higher than with SRM, or did not result in the development of a full failure mode. The main conclusions drawn from this comparative study are: 1) LEM is the least conservative method for all drained scenarios, and thus should be used with caution; 2) The failure mode for small cohesion intercepts c' varies between the methods, implying an uncertainty in the application of the methods; 3) The use of GIM requires further study.

Keywords: Slope Stability Analysis, Strength Reduction Method, Gravity Increase Method, Limit Equilibrium Method, Finite Element Limit Analyses

1. INTRODUCTION

Stability of slopes in cohesive soil has an important role of spatial planning of today, with both densification of urban areas as well as continuous maintenance of existing and construction of new infrastructure. The most commonly used methods for slope stability analyses are based on either kinematical or statical assumptions, such as limit equilibrium method and limit analysis, and are most often only applicable for isotropic material models, even though in some programs built-in functions to account for anisotropy of the limiting strength exist. A more rigorous way to model the behaviour of the soil is to use the displacement-based FEA (Finite Element Analysis), with the benefit of having the ability to include advanced anisotropic material models and strain softening, as needed for modelling sensitive clays.

This paper presents a case study where four methods of analyses for slope stability are applied for drained and undrained analyses with Mohr-Coulomb failure criteria. The case study is the initial result of a research project where numerical tools are planned to be developed to account for the effects of the climate change on the response of slopes in sensitive clay.

2. METHODS FOR SLOPE STABILITY ANALYSES

Stability of slopes is commonly evaluated by the Limit Equilibrium Method (LEM) where an assumed sliding mass is discretized in to vertical slices for which force and/or moment

equilibrium is calculated for each slice and the total mass, e.g. [1, 2]. The value of the stability in LEM is then defined as the ratio of the shear strength along the slip surface over the shear stress for at the same surface, the Factor of Safety (FoS), as defined by [3]. This method requires an iterative process to identity the size and location of the most critical slip surface. However, the method only considers circular (or pre-defined) slip surfaces, and assumes a constant mobilised shear strength along the slip surface of each slice. This could lead to an over- or underestimation of the stability, as well as the critical slip surface may be overlooked.

Other methods of analyses have been recently developed to for slope stability. This study will look at three alternatives to LEM: Discontinuity Layout Optimization (DLO), Finite Element Limit Analysis (FELA) and displacement-based Finite Element Analysis (FEA). The three methods simulate the soil mass either as a continuum (FEA, FELA), or by representing the soil with a large number of sliding blocks connected by nodes (DLO) [4-5, 7].

DLO is based on the upper bound theorem of plasticity, according to which the safety factor is described as the rate of work due to external loads over the simultaneous work done by internal stresses [4]. FELA on the other hand, allows for calculation of both the upper and lower bound to obtain an interval for the safety factor, where the lower bound is defined as the static equilibrium of the soil [5], and the upper bound considers the kinematics. Both DLO and FELA are simple but effective methods that have shown good agreement in previous comparison with LEM, e.g. [6], for undrained analyses.

The failure mode in FEA is dictated by the material model and the (effective) stress state, resulting in a slip surface being located where the mobilised shear strength is lower than the applied shear stress. This method automatically fulfils both the static and kinematic conditions, in contrast to DLO and LEM. Another advantage of using FEA over LEM, DLO and FELA is the ability to adopt advanced material models that can include the development of effective stresses and mobilised strength in the slope, as discussed by [7-8], as a function of time, or as a result of the changing environmental conditions due to the climate change.

The safety factor is calculated in the three methods above (DLO, FELA and FEM) by adjusting the properties of each cell or sliding block until failure by either: (1) reducing the cohesion and friction angle simultaneously with the Strength Reduction Method (SRM) or (2) increasing the gravitational loads with the Gravity Increase Method (GIM). As a result, SRM gives a safety factor, similar to LEM, whereas GIM gives the gravity multiplier required for failure. The main benefit of SRM and GIM is the lack of assumption of the shape or location for the critical slip surface. However, GIM is the only method that does not require specified strength parameters, and thus can work with any constitutive model.

The material models used in this study are based on the models available in the commercial software used, where LEM with Morgenstern-Price method (GeoStudio 2019 version 10.0.1.1733), DLO (LimitState:GEO version 3.4.a.20820), FELA (OptumG2 version 2019.02.12) and FEA (PLAXIS 2018) are all performed with Mohr-Coulomb failure criteria for drained and undrained analyses. Software-specific anisotropic functions have not been considered, as well as strain softening of the sensitive clay is not modelled at this stage in order to keep the results directly comparable.

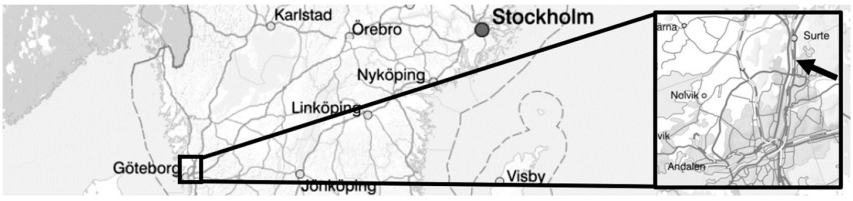


Figure 1. *Location of slope of interest, 10 km north of Gothenburg. (map from Lantmäteriet)*

3. DESCRIPTION OF CASE STUDY

The chosen slope is located by highway E45 at Göta River in the West of Sweden (Figure 1) with an inclination of 2H:1V and 13H:1V, of which the steepest part is partially located under water (Figure 2). Field investigations suggest a homogenous sulphide-bearing clay to >45 m depth with a sensitivity of 14-16. The pore pressure head is simplified in the model to be hydrostatic, at 1 m below the surface at the crest. The river is assumed to be 3 m deep. Material properties have been evaluated from fall cone tests, vane tests, direct simple shear tests and triaxial tests, of which the results are presented in Karlsson & Karstunen [9]. The friction angle has been assumed to be 36° for all soil layers, and the in situ coefficient of earth pressure at rest, K_0, have been evaluated by the combing Jaky's simplified formula with the empirical relation of Schmidt [10], assuming m = 0.6. The horizontal and vertical hydraulic conductivity assumed to be $k_x = k_y$ = 0.001 m/day and the drained analyses have been performed for three cohesion intercepts, c'=0.1 kPa, c'=0.5 kPa and c'=5 kPa.

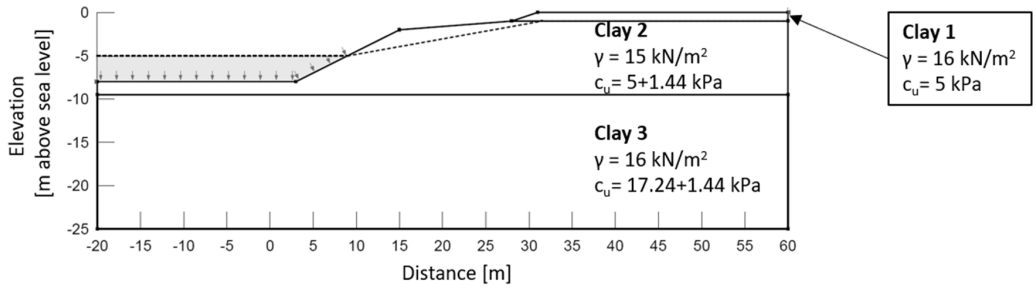


***Figure 2**. Geometry, stratification, density and undrained shear strength of the slope*

4. RESULTS AND DISCUSSION

The calculations have been performed with GIM and SRM for DLO, FELA and FEA, in addition to LEM. Results from the undrained analysis with the methods show good correlation for both the size and the location of the critical slip surface, as seen in Table 1 where a selection of the results are presented. The average obtained safety factor is 1.16 with a variation of up to 3%, which is considered to be most acceptable.

***Table 1.** Critical slip surface with corresponding safety factor for undrained conditions.*

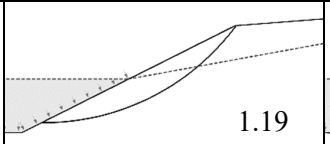
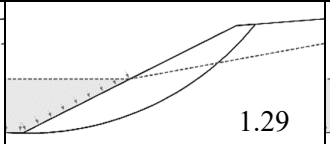
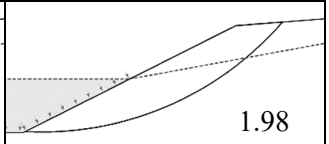
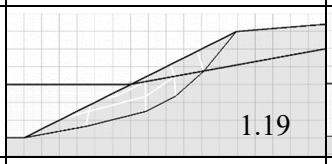
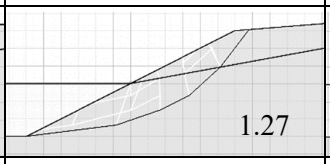
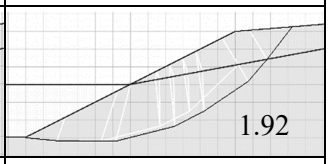
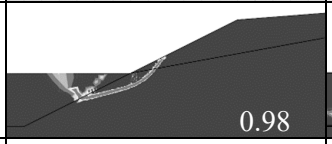
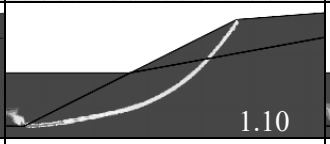
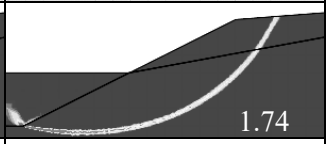
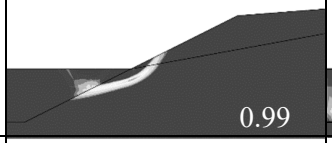
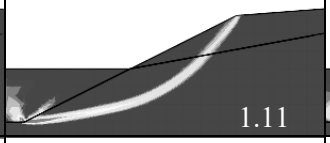
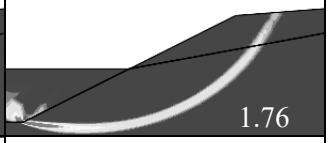
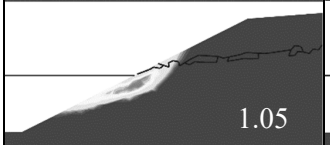
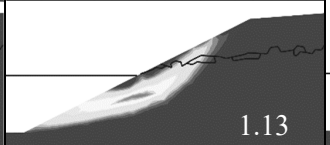
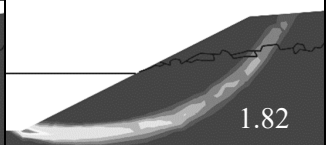
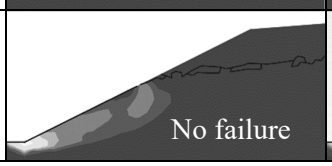
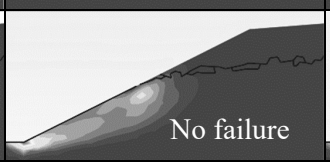
LEM, M-P: 1.19	FELA-LB-SRM: 1.16	FEA-SRM: 1.17
DLO-SRM: 1.18	FELA-UB-SRM: 1.17	FEA-GIM: 1.15

An overview of the results from the drained analyses with LEM and the SRM-implemented methods is presented in Table 2 together with the assumed values for the shear strength. Higher values are expected from FELA and FEA in a real case scenario, as in the analyses here, the two methods are applied without suction, in order to get comparable results with LEM and DLO. Furthermore, with FEA and FELA the slope stability analyses cannot be performed with

zero apparent cohesion, as the resulting mobilised strength at the surface would be zero. Thus, we investigated how much the assumed value for the cohesion intercept affects the results. The results in Table 2 indicate that one needs to be careful with the value chosen, as c' affects for example the mechanism and the volume of the failure mass. LEM and DLO show very similar result for all three scenarios. Systematically, LEM and DLO predict higher factors of safety than the FE -based methods (FELA and FEA). In terms of the mode of failure, the results by LEM and DLO are similar to FELA and FEA for higher values of c', even though the predicted factors of safety differ.

Results from FEA-GIM in drained analysis showed discrepancy of >100% from the other methods, and despite of ever increasing the coefficient of gravity, no full slip surface was developed to results in global failure. Similar performance was observed by Swan & Seo [8] and Sternik [11] when GIM was combined with Mohr-Coulomb and slopes of < 20-30 m of height in effective stress analysis. The phenomenon is associated with shallow depths, where the increase of gravity increases the shear strength of the soil rather than the loads bringing the slope to failure. In our case, the unit weight of the water in the river, which is a counter-balancing force, also increases. Modelling the river water as a load, however did not help. The same performance, i.e. no initiations of a clear failure mode, was also seen for FELA-GIM as well as DLO-GIM, which by definition of the failure criteria did not give a result.

Table 2. *Critical slip surface with corresponding safety factor predicted with SRM for drained conditions.*

Method	c'=0.1 kPa, φ'=36°	c'=0.5 kPa, φ'=36°	c'=5 kPa, φ'=36°
LEM, M-P	 1.19	 1.29	 1.98
DLO	 1.19	 1.27	 1.92
FELA, LB	 0.98	 1.10	 1.74
FELA, UB	 0.99	 1.11	 1.76
FEA, SRM	 1.05	 1.13	 1.82
FEA, GIM	 No failure	 No failure	 No failure

5. CONCLUSIONS

This paper describes a comparison between Limit Equilibrium Method (LEM), Discontinuity Layout Optimisation (DLO), Finite Element Limit Analysis (FELA) and displacement Finite Element Analysis (FEA) for undrained and drained analyses for a slope. The slope represents a typical case of a slope on sensitive clay along Göta River, Sweden. The study was performed with Mohr-Coulomb failure criteria, thus assuming the soil to be isotropic as commonly done in industry today. The safety factors for DLO, FELA and FEA was calculated with both Strength Reduction Method (SRM) and Gravity Increase Method (GIM). The latter has the advantage that it can be combined with any constitutive model. The results showed good correlation between the methods for total stress analyses (i.e. undrained analyses), but up to 20% difference between the four methods with SRM for drained analyses. The safety factors from FELA-GIM and FEA-GIM were unrealistically high, a behaviour that has been confirmed by previous literature [8, 11].

The main conclusions drawn from this comparative study are: 1) LEM is the least conservative method for all drained scenarios, and thus should be used with caution; 2) The failure mode for small cohesion intercepts c' varies between the methods, implying an uncertainty in the application of the methods; 3) The use of GIM requires further study. In the next stage, for the same slope, GIM will be applied in conjunction with an advanced constitutive model, as needed for representing the stability of a sensitive clay slope.

The study highlights the danger of implementing advanced climate-scenarios in calculation methods with in-built assumptions of failure mode or implementation of material models without cap model, as the safety factor varies substantially already without climate scenarios.

Effective stress analyses with advanced material models are essential to capture the climate-induced changes in strength of the soil, and its effect on the future slope stability. Such analyses cannot be done by exploiting the conventional LEM, which just like FELA and DLO suffer from the inability to account for changes in the soil response due to environmental loads. The latter include, in addition to pore pressure changes and erosion, in the Nordic situation also cyclic weather conditions affecting the dry crust and the shallow part of the slope. Phenomena such as extreme precipitation, increased number of yearly freeze-thaw and drying-wetting cycles, as well as the effect of vegetation or the lack of it, will affect the properties of the soil. A multi-physic approach will be needed, combined with probabilistic techniques.

The future research will initially look at six independent scenarios; 1) external erosion, 2) flooding, 3) changes in pore pressure due to precipitation, 4) freezing-thawing, 5) drying-wetting and 6) changes in temperature. Points 4) – 6) are of particular concern, as their cyclic nature is likely to affect the water content and soil fabric, and thereby increasing the depth or frequency of cracks in the upper part of the soil.

ACKNOWLEDGMENTS

Financial support by Swedish Geotechnical Society, FORMAS (2016-00834) and the Swedish Transport Administration (TRV 2016/106280) are greatly acknowledged.

REFERENCES

[1] Bishop, A.W., 1955. "*The use of the Slip Circle in the Stability Analysis of Slopes*", Géotechnique, 5(1):7-17, https://doi.org/10.1680/geot.1955.5.1.7.

[2] Morgenstern, N.R., Price, V.E., 1965. "*The Analysis of the Stability of General Slip Surfaces*", Géotechnique 15(1):79-93, https://doi.org/10.1680/geot.1965.15.1.79.

[3] Fellenius, W., 1926. "*Jordstatiska beräkningar med friktion och kohesion (adhesion) och under antagande av cirkulärcylindriska glidytor*". Kungl. Väg- och Vattenbyggarkåren 1851-1926, festskrift, Stockholm 22/12:79–127.

[4] Smith, C., Gilbert, M., 2007. "*Application of discontinuity layout optimization to plane plasticity problems*", Proceedings of the Royal Society, Series A, 463:2461-2484, https://doi.org/10.1098/rspa.2006.1788.

[5] Sloan, S.W., 2013. "*Geotechnical stability analysis*", Géotechnique 63(7):531-571, https://doi.org/10.1680/geot.12.RL.001.

[6] Hernvall, H., 2017. "*Clay slopes and their stability: An evaluation of different methods*", M.Sc Thesis, Chalmers University of Technology, Sweden, 64 pages.

[7] Zienkiewicz, O.C., Humpheson, C., Lewis, R.W., 1975. "*Associated and non-associated visco-plasticity and plasticity in soil mechanics*", Géotechnique 25(4):671–689, https://doi.org/10.1680/geot.1975.25.4.671.

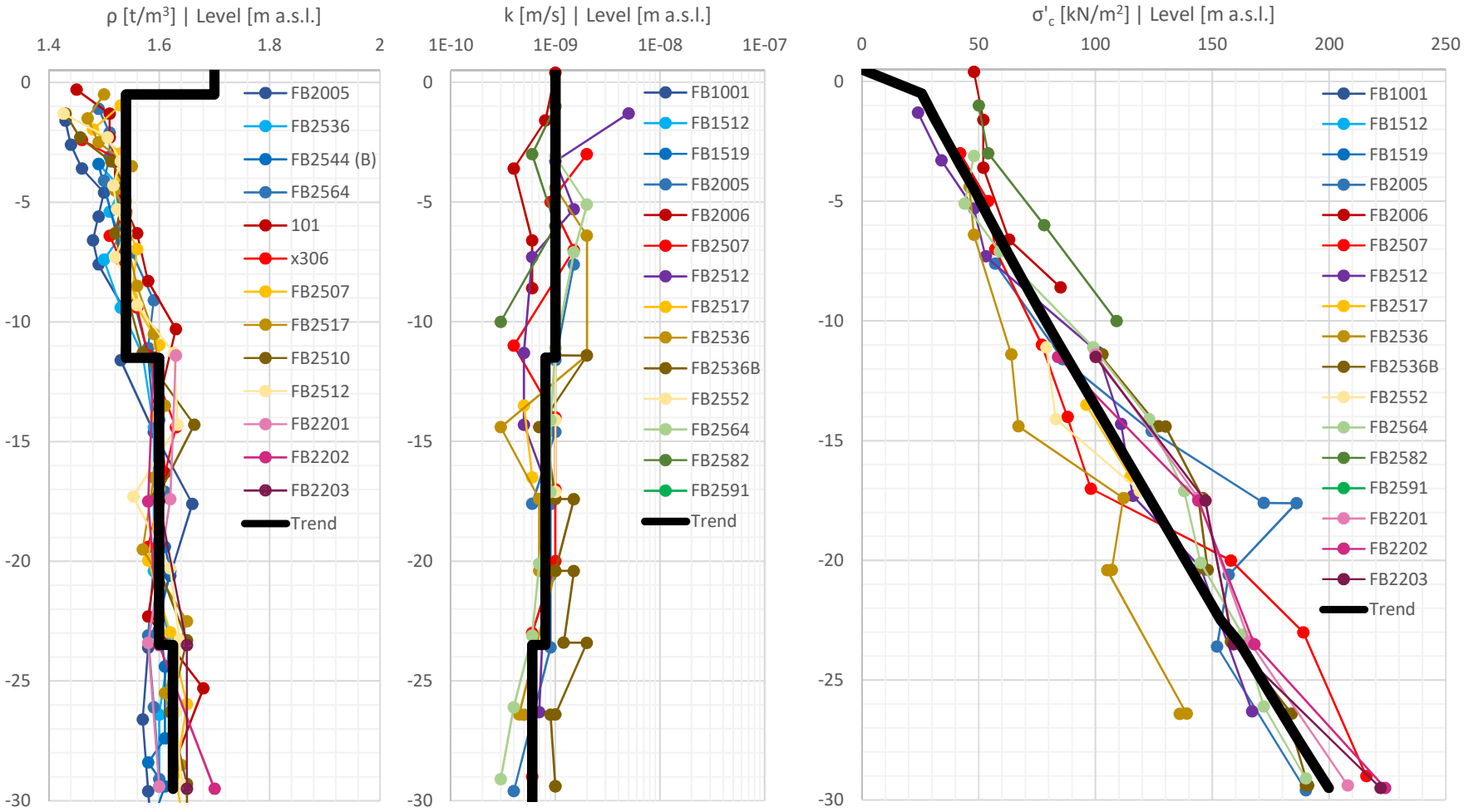
[8] Swan, C.C., Seo, Y-K., 1999. "*Limit state analysis of earthen slopes using dual continuum/FEM approaches*", International Journal for Numerical and Analytical Methods in Geomechanics, 23:1359-1371, https://doi.org/10.1002/(SICI)1096-9853(199910)23:12<1359::AID-NAG39>3.0.CO;2-Y.

[9] Karlsson, M., Karstunen, M., 2017. "*On the Benefits of Incorporating Anisotropy in Stability Analyses in Sensitive Clays*", In: Advances in Natural and Technological Hazards Research, 46:259-266, Springer, Netherlands, https://doi.org/10.1007/978-3-319-56487-6_23.

[10] Schmidt, B., 1966. "*Earth Pressures at Rest Related to Stress History*", Canadian Geotechnical Journal 3(4):239-242, https://doi.org/10.1139/t66-028.

[11] Sternik, K., 2013. "*Comparison of slope stability predictions by gravity increase and shear strength reduction methods*", Czasopismo Techniczne. Środowisko, R. 110, z. 1-Ś:121-130.

Appendix II: Summary of laboratory tests


ρ [t/m³] | Level [m a.s.l.]
1.4
1.6
1.8
2
0
-5
-10
-15
-20
-25
-30
FB2005
FB2536
FB2544 (B)
FB2564
101
x306
FB2507
FB2517
FB2510
FB2512
FB2201
FB2202
FB2203
Trend
k [m/s] | Level [m a.s.l.]
1E-10
1E-09
1E-08
1E-07
FB1001
FB1512
FB1519
FB2005
FB2006
FB2507
FB2512
FB2517
FB2536
FB2536B
FB2552
FB2564
FB2582
FB2591
Trend
σ'c [kN/m²] | Level [m a.s.l.]
0
50
100
150
200
250
FB1001
FB1512
FB1519
FB2005
FB2006
FB2507
FB2512
FB2517
FB2536
FB2536B
FB2552
FB2564
FB2582
FB2591
FB2201
FB2202
FB2203
Trend

Appendix III: Modelling of undrained shearing of soft natural clays

Modelling of undrained shearing of soft natural clays

lexandros L. Petalas[1,*], *Mats* Karlsson[1], and *Minna* Karstunen[1]

[1]Chalmers University of Technology, Dept. of rchitecture and Civil Engineering, Sweden

bstract. stress-strain response of soft natural clays is characterised by anisotropy, destructuration and rate-dependency. n accurate constitutive description of these materials should take into consideration all of the characteristics above. In this paper, two constitutive models for soft soils, namely the SCL Y1S and Creep-SCL Y1S models are used to simulate the undrained response of two soft natural clays, Gothenburg clay from Sweden and Otaniemi clay from Finland. The SCL Y1S model accounts for the e ect of inherent and induced anisotropy and destructuration, while the Creep-SCL Y1S accounts also for the creep and rate e ects. The model simulations are compared against triaxial compression and extension tests on anisotropically consolidated samples. The results demonstrate the need to incorporate all features represented in the Creep-SCL Y1S model when modelling structured natural clays.

1 Introduction

The mechanical response of soft natural clays is a ected by their micro-structure that is often anisotropic, and the apparent inter-particle bonding. Moreover, they exhibit rate-dependent behaviour. The initial anisotropy of marine clays is often developed under K_0-conditions (initial deposition, self-weight consolidation and aging), and the anisotropy evolves during subsequent loading, if the loading path di ers from the K_0-condition. In addition to the evolving anisotropy, when irrecoverable straining occurs and the particle cluster and contacts evolve, the inter-particle bonding degrades. This process is called destructuration [1].

Two constitutive models, namely SCL YS-1S [2] and Creep-SCL Y1S [3, 4] are used in this paper for simulating triaxial loading paths on two soft natural clays (Gothenburg and Otaniemi clays [5]). The elasto-plastic SCL Y1S model accounts for inherent and evolving anisotropy by utilising a rotational hardening law, proposed in [6]. In addition to anisotropy, the model accounts for bonding and destructuration by using the concept of an intrinsic yield surface [7]. Finally, the rate-dependent elasto-visco-plastic Creep-SCL Y1S model accounts not only for anisotropy, bonding and destructuration, but also for rate-e ects.

The paper is organised as follows: In Section 2 the two models are briefly presented, and the model parameters for the numerical simulations are discussed. In Section 3, data from triaxial compression and extension tests on anisotropically consolidated Gothenburg clay and their numerical simulations are presented. The e ects of destructuration, anisotropy and shearing rate are highlighted. The results demonstrate the need to incorporate all features represented in the Creep-SCL Y1S model. Consequently, in Section 4, three anisotropically consolidated undrained triaxial tests on Otaniemi clay are simulated, in which samples from the same depth have been exposed to different levels of anisotropic consolidation, before shearing to failure. These simulations highlight the need to account for the stress history and the degradation of bonding in the subsequent simulations.

2 Constitutive models and calibration

The SCL Y1S model [2] and the Creep-SCL Y1S [3, 4] model are presented schematically in triaxial space (Fig. 1) for the special case of a cross-anisotropic material with the main axis of the fabric coinciding with the principal stress directions in the triaxial test. The yield surface of SCL Y1S is a sheared ellipse [8], with the size defined by p'_m and the inclination by , a scalar measure of anisotropy for the special case of triaxial conditions. fabric tensor is used in the generalised formulation, (see [6]). The imaginary intrinsic yield surface represents the yield surface of the same soil, with the same void ratio and stress history, but without the bonds. The size of the intrinsic yield surface is controlled by the state variable p'_{mi}, with the same inclination as the the yield surface of the natural clay. The sizes of the two surfaces are related via state parameter χ by $p'_m = \chi p'_{mi}$.

Both the anisotropy, represented by , and the amount of bonding χ evolve due to irrecoverable straining. evolves towards a target value based on the current state of the soil, and hence the yield surface rotates, controlled by a rotational hardening law (see [6] for details). χ evolves from the initial value χ_0 towards zero due to destructuration. The elastic response of the model is assumed to be non-linear with a stress dependent elastic formulation, similar to the Modified Cam Clay model.

In the Creep-SCL Y1S model (Fig. 1), the yield surface is replaced by the Normal Compression Surface

e-mail: petalas@chalmers.se

© The Authors, published by EDP Sciences. This is an open access article distributed under the terms of the Creative Commons Attribution License 4.0 (http://creativecommons.org/licenses/by/4.0/).

(NCS), with the size defined by p'_p. n additional surface, representing the current (e ective) stress state (CSS) is used, with the size defined by p'_{eq}, and the same inclination as the NCS. The current stress state is always on the CSS. The distance of p'_{eq} with respect to p'_p relates to the magnitude of visco-plastic strains that are computed via an explicitly defined visco-plastic multiplier [9]. Creep-SCL Y1S does not predict purely elastic response, however, for $p'_{eq}<p'_p$, the magnitude of the predicted visco-plastic strain is very small. The rotational hardening and destructuration laws are the same as in the SCL Y1S model.

The model parameters are presented in Table 1. The calibration of the models are explained in detail in [2–4, 6, 10]. In this work, in order to investigate the e ect of destructuration, anisotropy and shearing rate, the complexity of the models is hierarchically increased. When $_0 = 0$, $\omega = 0$ and $\chi_0 = 0$ and the compressibility of the natural clay λ is used instead of the intrinsic value λ_i, the SCL Y1S model becomes equivalent to a Lode angle -dependent version of the Modified Cam Clay model (called MCC in the legends of the figures). When $\chi_0 > 0$ to account for the e ect of bonding, the model is an isotropic model with destructuration (called Structure in the legends). By using $\chi_0 > 0$, $_0 > 0$ and $\omega > 0$ the e ect of both destructuration and anisotropy are taken into account (called nisotropy in the legends). Finally, all the above and the rate e ects are taken into account via the Creep-SCL Y1S model (called Creep in the legends), which instead of λ_i uses the modified intrinsic compression index $\lambda^\star$, and the volumetric compression in the purely elastic range is represented by the modified swelling index $\kappa^\star$.

3 Undrained response of Gothenburg clay

In Figs. 2a and 2b the simulations of a triaxial compression and a triaxial extension test, respectively, are presented. The e ective stress and the void ratio of the soil after the anisotropic consolidation and the rate of undrained shearing are summarised in Table 2. It can be concluded that in triaxial shearing, the destrcucturation law plays a significant role. The equivalent MCC model cannot simulate the undrained softening response after the peak q. When anisotropy is taken into account via the rotational hardening law (nisotropy and Creep legends) the results become even more accurate, as far as the undrained triaxial extension response is concerned. The MCC model and the MCC with structure over-predict the purely elastic response as can be seen in Fig. 2bb. Finally, the Creep-SCL Y1S (Solid grey line) predicts a slightly higher peak due to the strain- rate e ect, but reproduces very accurately the anisotropic response and destructuration. This is suggesting that the assumed value for M_c is too high for the creep model, perhaps representing the peak rather than the critical state value.

Table 1. Value of the model parameters for Gothenburg and Otaniemi clays.

	Gothenburg Clay		Otaniemi clay
Parameter	SCL Y-1S	Creep SCL Y-1S	Creep SCL Y-1S
λ [-]	0.6	$\lambda^\star = 0.29$	$\lambda^\star = 0.26$
λ_i [-]	0.24	$\lambda_i^\star = 0.08$	$\lambda_i^\star = 0.063$
κ [-]	0.03	$\kappa^\star = 0.01$	$\kappa^\star = 0.012$
ν [-]	0.2	0.2	0.25
M_c [-]	1.4	1.4	1.3
M_e [-]	1.1	1.1	-
ω [-]	300	300	20
ω_d [-]	0.95	0.95	0.86
ξ [-]	8	8	15
ξ_d [-]	0.5	0.5	0.2
$_0$ [-]	0.54	0.54	0.5
χ_0 [-]	8	8	8
τ [days]	1	1	1
μ [-]	0.00125	0.00125	0.00125

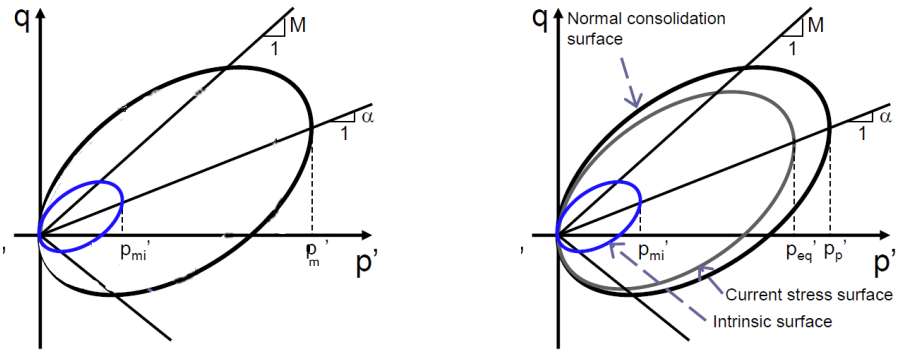
Table 2. ssumed initial conditions for triaxial compression and extension tests on Gothenburg clay. i: after consolidation, before shearing.

Test	e_i	$\sigma'_{a,i}$ [kPa]	$\sigma'_{r,i}$ [kPa]	K_0	OCR	Shear rate [mm/min]
TC	1.87	167	101.65	0.61	1.25	0.01
TE	1.95	176.61	101.65	0.58	1.25	0.01

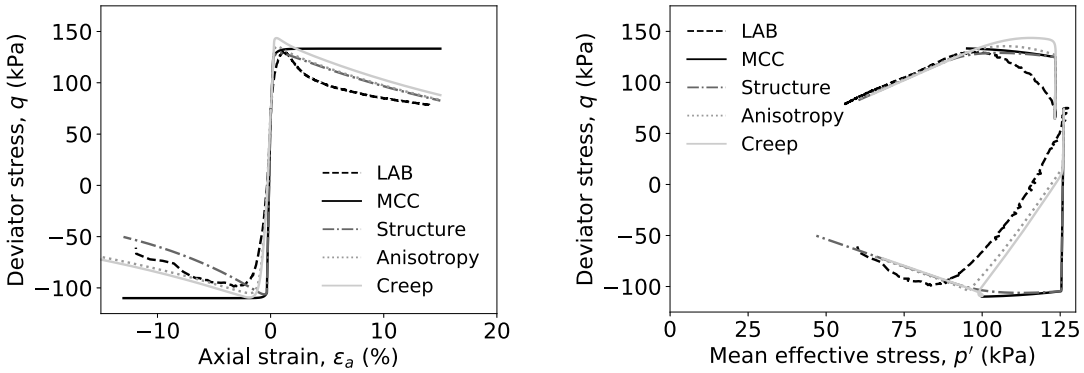
4 Undrained response of Otaniemi clay

Three undrained triaxial shear tests on natural Otaniemi clay are simulated with the use of the PL XIS finite element software and the Creep-SCL Y1S model as boundary value problems. The clay samples are extracted from the same depth and the Normal Compression Surface (NCS) is initialised by using the in-situ vertical e ective stress ($\sigma'_v = 25$) and K_{0NC} calculated via the Jaky's formula. The initial void ratio e_0 (before the anisotropic consolidation), the void ratio at the start of shearing e_i and the e ective stress state after the anisotropic consolidation, as well as the rate of shearing are summarised in Table 3.

The numerical simulations are performed in two stages. t the first stage the anisotropic consolidation is simulated. For the samples Ota2239 and Ota2240 the stress state after anisotropic consolidation is outside of the NCS, initialised by the apparent preconsolidation pressure of the natural clay, and thus, the NCS evolves during anisotropic consolidation. s the stress ratio used in the



ig. 1. Constitutive models. Left: SCL Y-1S; right: Creep-SCL Y1S.



(a) Stress-strain curves **(b)** Stress-path

ig. 2. Undrained triaxial shearing of Gothenbug clay and numerical simulations with evolving model complexity.

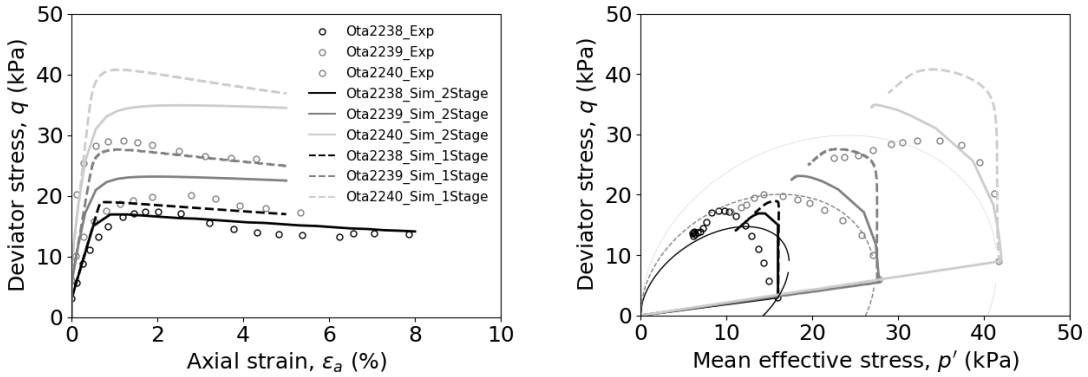
anisotropic consolidation di ers from the K_0 consolidation, NCS is also expected to rotate during consolidation.

t the second stage, undrained shearing is applied. The results of the simulations are presented in Figs. 3 and 3. There is good agreement of the results from the numerical analysis of Ota2238 test but the model overestimates the undrained strength for tests Ota2239 and Ota2240. Three additional dashed lines are presented in both Fig. 3 and 3 for additional simulations that do not take into account the anisotropic consolidation stage. In those simulations the inclination of the NCS estimated by the in-situ conditions is used (= 0.5) without taking into account any evolution during anisotropic consolidation. Moreover, the initial value of the destructuration parameter $\chi_0 = 8$ and it's evolution is also not taken into account. It can be concluded from Fig. 3 and 3 that not including the evolution of the state variables during anisotropic consolidation significantly decreases the accuracy of the predictions. The numerical simulations can be improved if more data for the initial inclination of the NCS and it's evolution are available.

Fig. 4a demonstrates how the model predicts the anisotropy decreases significantly during consolidation for Ota2289 and Ota2240, due to the high applied value of K_0 ≈0.8, and consequently NCS is predicted to rotates towards the isotropic state. During the undrained shearing anisotropy evolves again, with an increasing -value predicted. The bonding parameter χ (Fig. 4b) is also predicted to decreases significantly both during the anisotropic consolidation and the undrained shearing. Consequently, it is very important to simulate both stages in these triaxial tests as the initial consolidation will also change the initial state if the clay is allowed to yield during the consolidation.

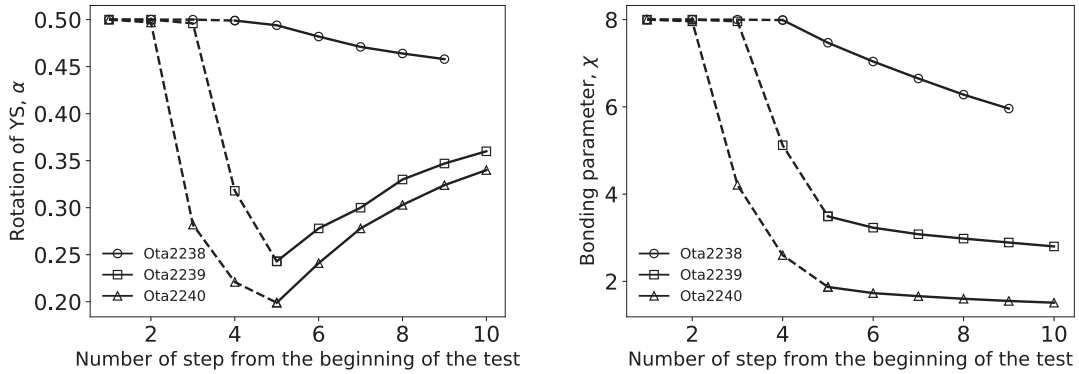
Table 3. Initial conditions for triaxial compression of Otaniemi clay. 0: before consolidation; i after consolidation, before shearing.

Test	e_0	e_i	q_i [kPa]	p'_i [kPa]	K_0	Shear rate [%/h]
Ota2238	3.28	3.14	3	15.9	0.83	0.63
Ota2239	3.47	2.76	6	27.7	0.82	0.64
Ota2240	3.32	3.32	9	41.7	0.81	0.061



(a) Stress-strain curves **(b)** Stress-path

ig. 3. Undrained shearing tests on Otaniemi clay and numerical simulations with Creep-SCL Y1S. Solid lines: Simulating both the anisotropic consolidation and the undrained shearing stages (2 stages). Dotted lines: Simulating only the undrained shearing stage (1 stage). Lab data after [5].



(a) nisotropy **(b)** Structure

ig. 4. Undrained shearing tests on Otaniemi clay [5] and numerical simulations with Creep-SCL Y1S. Stage 1 (Dashed lines): anisotropic consolidation; stage 2 (Solid lines): undrained shearing.

5 Conclusions

In this work, the important role of the evolution of anisotropy and destructuration of soft structured clays is demonstrated based on simulations on undrained triaxial shearing tests of Gothenburg and Otaniemi clays. Simulations of Gothenburg clay by hierarchically increasing the model complexity demonstrate that features such as anisotropy and destructuration are important to account for in modelling the clay response over the whole e ective stress range, The simulations of Otaniemi clay, on the other hand highlight the need to account for the changes in the state of the soil during the initial consolidation.

The financial support by the Swedish Research Council FOR-M S (contract number 2016-00834) and by Swedish Transportation authority under the umbrella of BIG (Brach Collaboration in Ground, contract number TRV 2016/106280) is greatly acknowledged.

References

[1] S. Leroueil, P.R. Vaughan, Geotechnique **3**, 467 (1990)

[2] M. Koskinen, M. Karstunen, S. Wheeler, *Modelling destructuration and anisotropy of a natural clay*, in *5th European Conf. Numerical Methods in Geotechnical Engineering*, edited by P. de L'ENPC/LCPC (Paris, 2002), pp. 11–20

[3] N. Sivasithamparam, M. Karstunen, P. Bonnier, Computers and Geotechnics **69**, 46 (2015)

[4] J. Gras, N. Sivasithamparam, M. Karstunen, J. Dijkstra, Computers and Geotechnics **90**, 164 (2017)

[5] M. Koskinen, Ph.D. thesis, alto University (2014)

[6] S. Wheeler, . Naatanen, M. Karstunen, M. Lojander, Canadian Geotechnical Journal **40**, 403 (2003)

[7] . Gens, R. Nova, *Conceptual bases for a constitutive model for bonded soils and weak rocks*, in *In-*

ternational Symp. on Hard Soils-Soft Rocks (thens, 1993), pp. 485–494

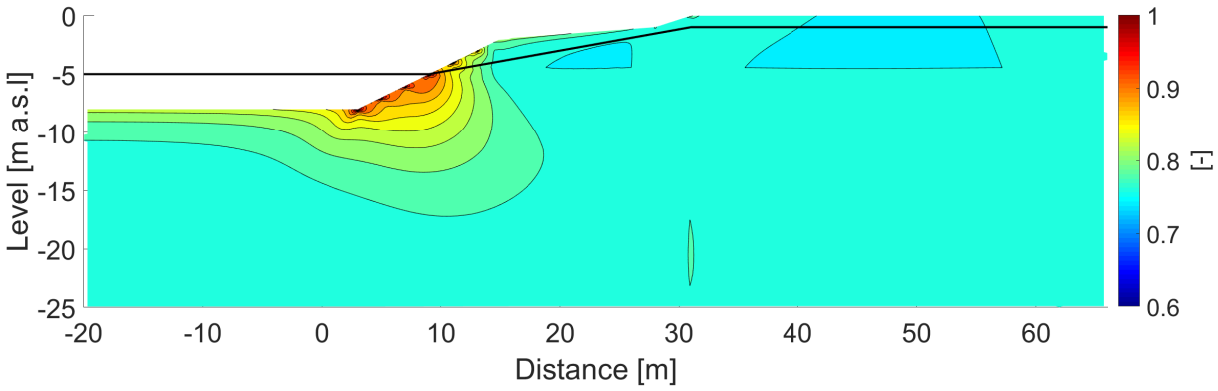
[8] Y.F. Dafalias, Mechanics Research Communications **13**, 341 (1986)

[9] G. Grimstad, S. . Degago, S. Nordal, M. Karstunen, cta Geotechnica **6**, 69 (2010)

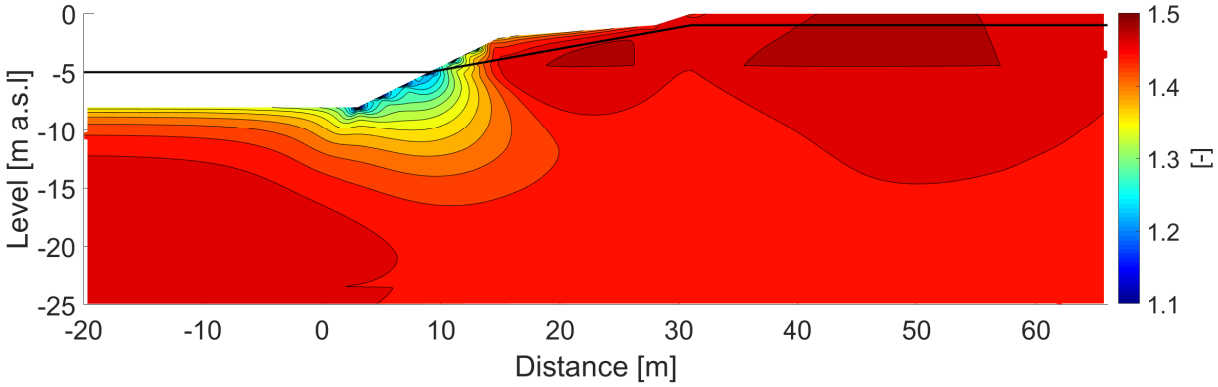
[10] M. Karstunen, H. Krenn, S. Wheeler, M. Koskinen, R. Zentar, International Journal of Geomechanics **9**, 153 (2009)

Appendix IV: Will be published separately during 2021.

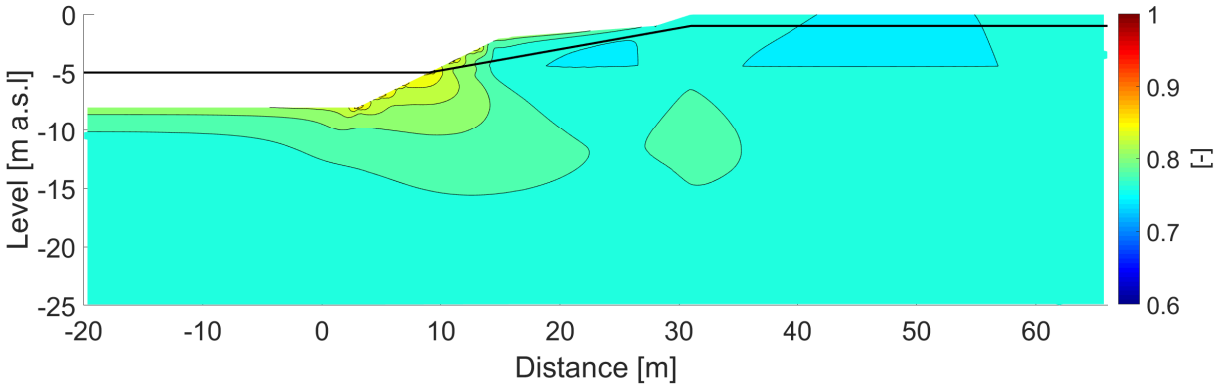
Appendix V: Results from numerical simulations



Rotation of yield surface, α_{xx} [-]



Rotation of yield surface, α_{yy} [-]



Rotation of yield surface, α_{zz} [-]

BIG – Branschsamverkan i grunden
Forskningsprogram för effektiv och säker grundläggning av vägar och järnvägar

BIG

BIG – Branschsamverkan i grunden - är ett forskningsprogram för effektiv och säker grundläggning av transportsystemets infrastruktur. Programmet etablerades under senhösten 2013, och påbörjade sin verksamhet den 1 januari, 2014.

Målsättningen är att sänka kostnader för byggande och underhåll av transportsystemets infrastruktur genom ett långsiktigt och systematiskt utvecklingsarbete inom geoteknikområdet.

I BIG samverkar Trafikverket, Chalmers tekniska högskola, Luleå tekniska universitet, Kungliga tekniska högskolan och Statens geotekniska institut.

Resultat från BIG projekt publiceras i vetenskapliga artiklar och parternas egna rapportserier. Alternativt så publiceras rapporterna i denna gemensamma BIG rapport serie.

Publicerade rapporter

A2014:03	Deformationer i undergrund – Litteratursammanställning och analys
A2014:07	Grundvattensänkning i morän
A2014:13	Höghastighetsspår i Sverige – på bank
A2014:14	On the fundamental relation between soil creep and cyclic pile-soil response
A2017:10	Effects of climate change on slopes in sensitive clay